EXPERIMENT 1

Response of soil CO_2 efflux and net ecosystem exchange to rainfall variability in wheat field

ลิขสิทธิ์มหาวิทยาลัยเชียงใหม่
Copyright© by Chiang Mai University
All rights reserved

Sub-experiment 1: Short-term response of total soil CO_2 efflux and heterotrophic respiration to rainfall in a winter wheat field

INTRODUCTION

Rising atmospheric carbon dioxide concentration ($[CO_2]$) and temperature alter the oceanic and the terrestrial carbon cycle, causing positive feedbacks to the global climate (IPCC, 2007). Soil CO_2 emissions play a significant role in the terrestrial global carbon cycle because the soil is the largest active carbon (C) pool in terrestrial ecosystems, releasing approximately 68-75 Pg C $year^{-1}$ to the atmosphere (Raich and Schlesinger, 1992). This pool is in turn influenced by both temperature and precipitation, two critical factors which involve in the regulation of soil CO_2 emissions (Lloyd and Taylor, 1994; Yuste *et al.,* 2003; Huxman *et al.,* 2004; Tang *et al.,* 2005; Frank *et al.,* 2006). Therefore, changes in soil CO_2 efflux in response to environmental change can play an important role on the carbon budget (Andrews *et al.,* 1999; Schlesinger and Andrews, 2000). However, gains and losses of soil carbon are typically highly variable and difficult to predict. To understand the factors underlying temporal variations in the magnitude of the soil CO_2 efflux is therefore critical to produce a more robust estimate of soil emissions in the terrestrial carbon budget.

Soil CO_2 efflux consists mainly of autotrophic (including associated respiration from mycorrhizae) and heterotrophic respiration (microbes and soil fauna). The separation of soil CO_2 efflux into root and heterotrophic respiration is of particular relevance in identifying the sensitivity of soil carbon cycling and

ลิขสิทธิ์มหาวิทยาลัยเชียงใหม่
Copyright© by Chiang Mai University
All rights reserved

sequestration to environmental change. *In situ* measurements of heterotrophic respiration are inherently difficult since there are no effective methods of partitioning soil CO_2 efflux contributed by the roots from that contributed by the microbial organisms without disturbing the roots (Hanson *et al.,* 2000; Buchmann, 2000). Currently, the root exclusion (trenching) method provides realistic estimates of heterotrophic respiration in forest and grassland soils (Lee *et al.,* 2003; Li *et al.,* 2006; Ngao *et al.,* 2007). However, heterotrophic respiration using the root exclusion method has yet to be quantified in agricultural soils as shown in the present study.

Rainfall variability (including pattern, amount and timing) was proposed as a key mechanism controlling soil CO_2 efflux in many forest soils (Lee *et al.,* 2002; Lee *et al.,* 2004; Tang *et al.,* 2005; Jarvis *et al.,* 2007) and grassland soils (Liu *et al.,* 2002; Chen *et al.,* 2008). It has been observed that rainfall events lead to an increase of soil CO_2 efflux capable of significantly influencing the annual carbon budget (Lee *et al.,* 2002; Yuste *et al.,* 2003; Xu *et al.,* 2004). Despite previous studies relating soil water content to soil CO_2 emissions, there has been a paucity of studies elucidating the effect of rainfall on soil CO_2 efflux in agricultural soils. Neglecting such significant quantities of CO_2 efflux from soils following rainfall can underestimate soil CO_2 emissions (Liu *et al.,* 2002; Smart and Peñuelas, 2005). In agricultural ecosystems with fast-growing vegetation, the wide range of available water from either rainfall or irrigation contributes to equally variable microbial activity (Koçyiğit and Rich, 2006).

The effect of rainfall on soil CO_2 efflux has recently been recognized (Liu *et al.,* 2002; Jassal *et al.,* 2005; Smart and Peñuelas, 2005). Yet, how soil CO_2 efflux responds to rainfall characteristics still needs to be better understood (Huxman *et al.,* 2004; Xu *et al.,* 2004). Generally, the response of soil CO_2 efflux to rainfall is rapid.

ลิขสิทธิ์มหาวิทยาลัยเชียงใหม่
Copyright© by Chiang Mai University
All rights reserved

Laboratory observations by Lee *et al*. (2004) indicated that the response of soil CO_2 efflux occurs within 1hr after rain. Soil CO_2 efflux measurements taken over short periods in daytime conditions make data analysis challenging for periods with significant precipitation because the data cannot be assumed to represent the daily mean soil CO_2 efflux (Liang *et al.,* 2004). Snapshot data collected weekly or even bi-weekly may not provide an accurate and dynamic measure of soil CO_2 efflux. Such studies often miss the peaks in CO_2 efflux following rainfall due to the coarse temporal resolution of the field measurements, leading to large uncertainties in total seasonal and annual values of soil CO_2 efflux (Tang *et al.,* 2003). This suggests the need for soil CO_2 efflux data to be gathered at a finer temporal resolution.

This study presents high-frequency and high-precision observations of soil CO_2 efflux in a wheat field. Continuous measurement of soil CO_2 concentration gradients was conducted to capture the rapid response of soil CO_2 efflux to rainfall events and soil water content. The root exclusion method was also used to quantify how heterotrophic respiration responds to rainfall events. The objectives of this study were: (1) to examine mechanisms of soil CO_2 efflux following rainfall during the growing season of wheat; (2) to identify soil temperature and soil water content that drive the variation of soil CO_2 efflux.

ลิขสิทธิ์มหาวิทยาลัยเชียงใหม่
Copyright© by Chiang Mai University
All rights reserved

MATERIALS AND METHODS

The research was carried out at the University of Georgia's Southwest Georgia Research and Education Center in Plains, GA, USA during November 2006 to early May 2007.

Site description

The study was conducted at the University of Georgia's Southwest Georgia Research and Education Center in Plains, GA, USA (32.050° N, 84.367° W; elevation 152 m). Mean annual precipitation is 1246.1 mm and mean annual temperature is 24.2 °C. Winter wheat *(Triticum aestivum* L., var. AgSouth 2000*)* was planted in November 2006. Before sowing, the soil was plowed for land preparation. Sowing density of winter wheat was 56 kg per ha at a 0.06 m spacing. Basal fertilizer of N, P_2O_5, K_20 (4-22-6) was applied at 448 kg per ha during planting. Before heading, 56 kg per ha of urea was applied and there was no irrigation applied in the growing season during this study. The field was harvested on 14 May 2007 and wheat yield was about 5043.75 kg per ha.

Soil type is a sandy clay loam. The soil for planting wheat is composed of 52% sand, 20% silt and 28% clay with a bulk density of 1.03 and 2.24% of organic matter.

ลิขสิทธิ์มหาวิทยาลัยเชียงใหม่
Copyright© by Chiang Mai University
All rights reserved

Soil CO_2 efflux measurements

Soil CO_2 efflux was measured by using soil CO_2 gradient measurement systems in a wheat site over the period from February to May 2007. Soil CO_2 efflux

was also measured at two locations inside a trenched plot (or root exclusion experiment) and an untrenched location (Fig. 2.1). A small plot 3m x 3m for the trenched method was established in an open space created in the field by digging a trench 0.40 m deep and 1.2 m wide. The inside wall of the trench was lined with a polyethylene sheet and the trench was refilled the soil back according to its original soil profiles to minimize disturbance. The trench cut down most live roots that extended into the plot. The barrier sheets were also installed to inhibit future root growth. The trenched plot was then kept free of any vegetation by periodic manual removal. Thus, it can be assumed that there were no root influences within this plot. The untrenched plot was set up at a lateral distance of 3 m away from the center of the trenched plot.

In this study, total soil CO_2 efflux is defined as the combination of root respiration of living root tissue and the respiration of symbiotic mycorrhizal fungi and associated microorganisms as in the untrenched plot. Heterotrophic respiration is defined as the respiration of soil microorganisms and microorganisms not directly under the influence of the live root system as in trenched plot.

In all plots were installed solid-state infrared gas analyzers (GMP343, Vaisala Inc., Finland) to continuously monitor soil CO_2 concentration profiles buried at depths of 0.04 and 0.08 m during the vegetation period at the center of trenched plot and in the soil beneath a wheat canopy in the untrenched plot. The probe is 0.18 m in length and 0.055 m in diameter. Before installation, the sensors were covered with a sintered PTFE (polytetrafluoroethylene) filter and a cap made of POM (polyoxymethylene) with a diffusion slot enabling gas exchange between the soil and the probe and protecting the probe from water. The sensors were installed in a horizontal face of a

ลิขสิทธิ์มหาวิทยาลัยเชียงใหม่
Copyright© by Chiang Mai University
All rights reserved

soil pit excavated at the field with the different soil layers kept separately. Then, soils layers were placed back in the same order to minimize the disturbance. Fick's gradient diffusion equation was applied to calculate the CO_2 efflux from the soil.

$$F_z = -D_s \frac{dC}{dz} \quad (1)$$

where F_z is the soil CO_2 efflux, D_s is the gaseous CO_2 diffusion coefficient in the soil that varies with soil, C is the CO_2 mole concentration at a certain depth of the soil, and z is the depth. For flux determination, the gradient was approximated by discrete differences ΔC and Δz.

Diffusivity was computed with the Moldrup model (Moldrup *et al.,* 2000).

$$\frac{D_s}{D_a} = \frac{\varepsilon}{\phi}^{2.5} \quad (2)$$

where D_a is the CO_2 diffusion coefficient in the free air, ε is the volumetric air content (air-filled porosity), ϕ the porosity or sum of the volumetric air content ε and the volumetric water content (θ).

Environmental measurements

Soil temperature was measured with thermocouples (type E, Omega Engineering Inc., CT) at depths of 0.04, 0.08, 0.12 and 0.30 m near the CO_2 concentration sensors but at a lateral distance of 0.08 m away from the probe. Volumetric soil water content was measured at depths of 0-0.04, 0.04-0.08 and 0.08-0.30 m at the same location using time-domain reflectometers, TDR (CS616,

ลิขสิทธิ์มหาวิทยาลัยเชียงใหม่
Copyright© by Chiang Mai University
All rights reserved

Campbell Scientific Inc., Logan, UT). Rainfall was measured above the canopy with a tipping bucket rain gauge (TE525, Campbell Scientific Inc., Logan, UT). The observation was taken every second and stored as 5 min average in a datalogger (CR1000, Campbell Scientific Inc., Logan, UT). In addition, soil bulk density was also measured.

Half-hourly cumulative rainfall was measured above the canopy with a tipping bucket rain gauge with a resolution of 0.1 mm (TE525, Campbell Scientific Inc., Logan, UT). The 12 soil samples (0-0.15 m depth) were collected using a soil corer. The soil sample was weighed, dried at 105 °C for at least 48 hr, and then re-weighed to calculate soil porosity.

Figure 2.1 The solid-state infrared gas analyzers (GMP343) set up at the center of trenched plot (Left) and in the soil beneath a wheat canopy in the untrenched plot (Right).

ลิขสิทธิ์มหาวิทยาลัยเชียงใหม่
Copyright© by Chiang Mai University
All rights reserved

Data analysis

Generally, soil temperature and soil moisture are considered the most influential environmental factors controlling soil CO_2 efflux. The relationship between soil CO_2 effluxes *F(T)* and soil temperature (*T*) was represented by:

$$F(T) = ae^{bT} \quad (3)$$

where *a* and *b* are coefficients estimated by the non-linear regression, *a* denotes the reference soil CO_2 efflux at 0 °C and *b* provides an estimate of the Q_{10} coefficient. Q_{10} is the dependence of soil CO_2 efflux on soil temperature and was calculated according to the following equation:

$$Q_{10} = e^{10b} \quad (4)$$

To examine the response of the soil CO_2 efflux on soil water content, the non-linear regression was applied as the quadratic function.

$$F(\theta) = a + b\theta + c\theta^2 \quad (5)$$

where $F(\theta)$ is soil CO_2 efflux ($\mu molm^{-2}s^{-1}$), θ is the volumetric soil water content (m^3m^{-3}) and a, b and c are coefficients estimated by non-linear regression.

To examine the response of the soil CO_2 efflux on soil temperature and water content, the non-linear regression was used.

$$F = ae^{bT}\, e^{c\theta + d\theta^2} \quad or \quad \ln(F) = \ln(a) + bT + c\theta + d\theta^2 \quad (6)$$

ลิขสิทธิ์มหาวิทยาลัยเชียงใหม่
Copyright© by Chiang Mai University
All rights reserved

where F is soil CO_2 efflux (μmol $m^{-2}s^{-1}$), T is the soil temperature (°C), θ is the volumetric soil water content (m^3m^{-3}) and *a, b, c* and d are coefficients estimated by non-linear regression.

All statistical analyses were performed using Origins package, Version 7 (Origins Cooperation, Massachusetts, USA). Unless otherwise stated, significant differences of all statistical test were evaluated at the level $\alpha = 0.05$.

ลิขสิทธิ์มหาวิทยาลัยเชียงใหม่
Copyright© by Chiang Mai University
All rights reserved

RESULTS

Daily variation in soil CO_2 efflux, soil temperature and soil water content

The variation of daily mean soil CO_2 efflux and rainfall in the untrenched plot with roots and in the trenched plot without root in wheat field for 51 days from March to April 2007 (the day of year (DOY) from 60 to 120) are shown in Figure 2.2. The daily mean soil CO_2 efflux estimated from soil CO_2 concentration profiles in the untrenched plot were higher than in the trenched plot during DOY 60-91. Daily soil CO_2 efflux changed from 0.69 to 4.17 μmol $m^{-2}s^{-1}$ in the untrenched plot and from 0.45 to 2.95 μmol $m^{-2}s^{-1}$ in the trenched plot, respectively. While, soil CO_2 efflux in the trenched plot was higher than in the untrenched plot after the two rainfall events.

Fig. 2.2b and 2.2c shows the daily variations in volumetric soil water content at 0.04-0.08 m and soil temperature at 0.08 m. Daily mean volumetric soil water content was lower in the untrenched plot than in the trenched plot and then increased become highest at 0.20 m^3m^{-3} after rainfall. Volumetric soil water content continuously decreased from DOY 67-90 with a minimum of 0.12 m^3m^{-3} in the untrenched plot and 0.16 m^3m^{-3} in the trenched plot. The rain events on DOY 74-75 did not increase soil water content in both plots, but it rapidly increased after two rain events on DOY 91 and DOY 104-105. Overall, soil temperature in the trenched plot was a little higher than in the untrenched plot. Daily mean soil temperature peaked at 24.0 °C in the untrenched plot and 26.4 °C in the trenched plot on DOY 117. The patterns of daily change in soil temperature and volumetric soil water content in the trenched plot were similar to that of the untrenched plot.

ลิขสิทธิ์มหาวิทยาลัยเชียงใหม่
Copyright© by Chiang Mai University
All rights reserved

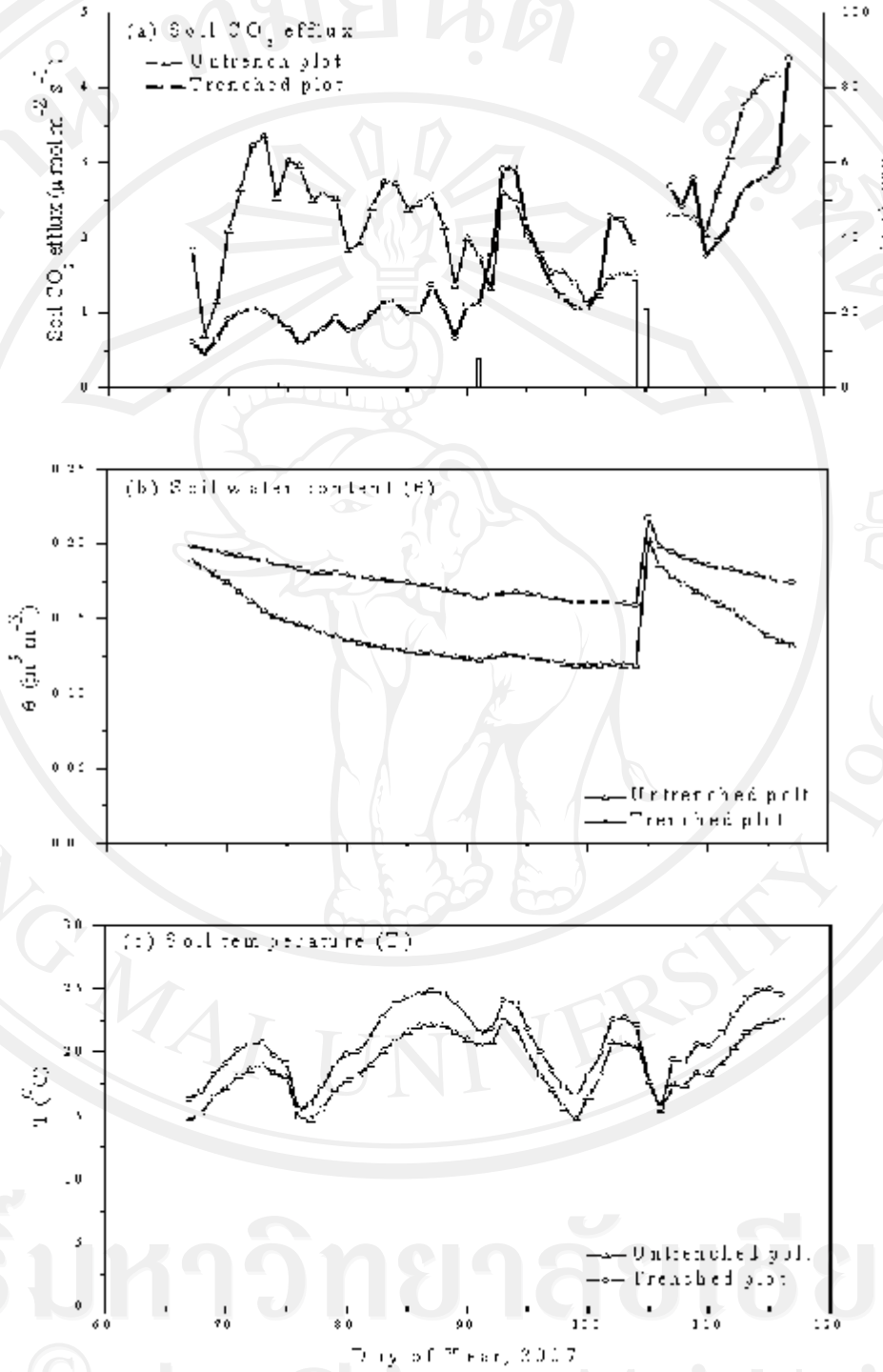

Figure 2.2 Daily variations in soil CO_2 efflux (a) in relation to soil temperature (b), volumetric soil water content (c) and rainfall in the untrenched and trenched plots.

ลิขสิทธิ์มหาวิทยาลัยเชียงใหม่
Copyright© by Chiang Mai University
All rights reserved

Response of CO_2 concentration and soil CO_2 efflux during and following rainfall

(a) Total soil CO_2 efflux in the untrenched plot

In order to examine how CO_2 concentration, [CO_2], varies in soil air pores during rainfall events, the soil data from 30 March to 6 April (DOY 89 to DOY 96) was used. Soil CO_2 concentration at depths of 0.04 and 0.08 m showed immediately increased during an 8-hr period, following a 7.8 mm rainfall event in the untrenched plot (Fig. 2.3a). Soil CO_2 concentration at the depth of 0.04 m rapidly increased from 1,140 to 2,685 ppm during the rainfall event in the untrenched but the increase was delayed at the depth of 0.08 m. Subsequently, a rapid and substantial decrease in soil CO_2 efflux occurred during the rainfall. The soil CO_2 efflux gradually decreased within minute following rain, and was about 37% lower than the efflux before rain. This corresponded with drop in soil temperature due to water content infiltration in to the soil. As calculations using soil water content between 0.04-0.08 m showed that the diffusivity also decreases following rain (Fig. 2.3a). Immediately after rain, soil CO_2 efflux increased gradually and was 1.27 times greater than the efflux before rain. The high peak of soil CO_2 efflux lasted for more than 2 days (period I) despite the gradual decline in soil water content (Fig. 2.3a). However, soil CO_2 efflux returned to approximately the efflux levels (period II) before rain over 5 days and decreased with decreasing soil water content.

ลิขสิทธิ์มหาวิทยาลัยเชียงใหม่
Copyright© by Chiang Mai University
All rights reserved

(b) Heterotrophic respiration in the trenched plot

Sudden increase in soil water content due to rainfall resulted in significant increases in soil CO_2 concentration at both depths in the trenched plot. Soil CO_2 concentration at the depth of 0.04 and 0.08m slow increased from 935 to 1,386 ppm and from 1,789 to 2,029 ppm during the rainfall event. The increase, however, was delayed when compared with the efflux in the untrenched plot (Fig. 2.3b). In contrast, the soil CO_2 efflux gradually decreased, and was about 13% lower than the efflux before rain. However, immediately after rainfall the soil CO_2 efflux increases was 2.11 times greater than the efflux before rain and then declined. This increased in soil CO_2 efflux after rainfall was also accompanied by increase in soil temperature. The peak of soil CO_2 efflux (period I) lasted for more than 2 days and the increased in soil CO_2 efflux was corresponded with a decreased in soil water content. However, soil CO_2 efflux after the peak (period II) returned to approximately the efflux levels before rain within 5-6 days. The decline in soil CO_2 efflux showed similar trend to drop in soil water content.

ลิขสิทธิ์มหาวิทยาลัยเชียงใหม่
Copyright© by Chiang Mai University
All rights reserved

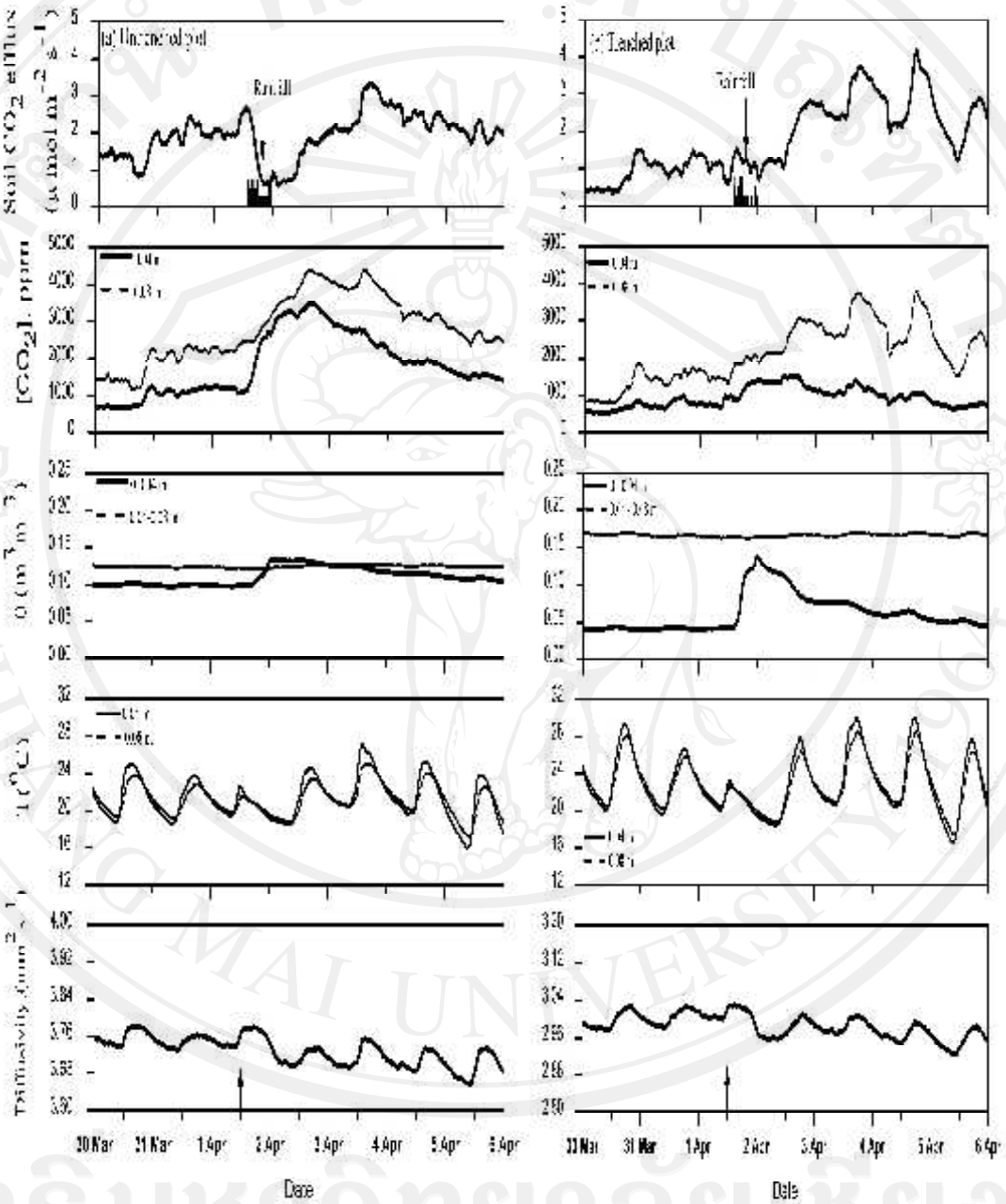

Figure 2.3 Effect of a natural 7.8-mm rainfall event on soil CO_2 efflux, soil CO_2 concentration at 0.04 and 0.08 m depths [CO_2], soil water content at 0-0.04 m and 0.04-0.08 m depths (θ), soil temperature at 0.04 and 0.08 m depths (T), and CO_2 diffusivity in the untrenched (a) and trenched plots (b). Arrow indicate rainfall event.

ลิขสิทธิ์มหาวิทยาลัยเชียงใหม่
Copyright© by Chiang Mai University
All rights reserved

The relationship between CO_2 concentration and soil CO_2 efflux with soil temperature and soil water content

Increase in soil CO_2 concentration during at time associated to soil rewetting after rainfall, soil was hot and dry for long times (23 days without rain) in both plot. Underground deep remained some soil water content, although surface appears very dry in both plots (Fig. 2.3). Therefore, 7.8 mm of rainfall could infiltrate through the shallow depth but could not move deeper because the deeper layer still remained some soil water content. To support reason as comparison soil water content level between 0.04 and 0.08 m (Fig 2.3). The infiltrating water was replaced of CO_2 gaseous in the soil porosity of the shallow layer. The result show the over high CO_2 concentration during rainfall and drop in soil CO_2 efflux. Later on the decrease in soil CO_2 efflux might have result form the restriction of soil porosity by rainfall infiltration, reducing soil air-fill pore space and soil CO_2 diffusivity.

In order to examine the effect of rainfall on soil CO_2 efflux, soil CO_2 efflux plotted against soil temperature and water content using half-hourly data recorded on day before and after rainfall event. Soil CO_2 efflux increased exponential with increasing temperature after rainfall (period I and II) in the untrenched (Fig. 2.4a) and the trenched (Fig. 2.5a) plots, excluding the soil CO_2 efflux before and during rainfall, suggesting that sensitivity of soil CO_2 efflux to temperature increased with water addition. Additionally, the poor relationships between soil CO_2 efflux and soil water content occurred before and during rainfall in both plots (Fig. 2.4b and 2.5b). After rainfall, soil CO_2 efflux increased with decreasing soil water content by drainage of the upper soil layer and then soil CO_2 efflux decline to pre-rainfall level. These results indicated that change in soil water condition by rainfall severely promote the ability

ลิขสิทธิ์มหาวิทยาลัยเชียงใหม่
Copyright© by Chiang Mai University
All rights reserved

of respiration to respond to changing temperature. Soil temperature pays a secondary role to rainfall in governing soil CO_2 efflux

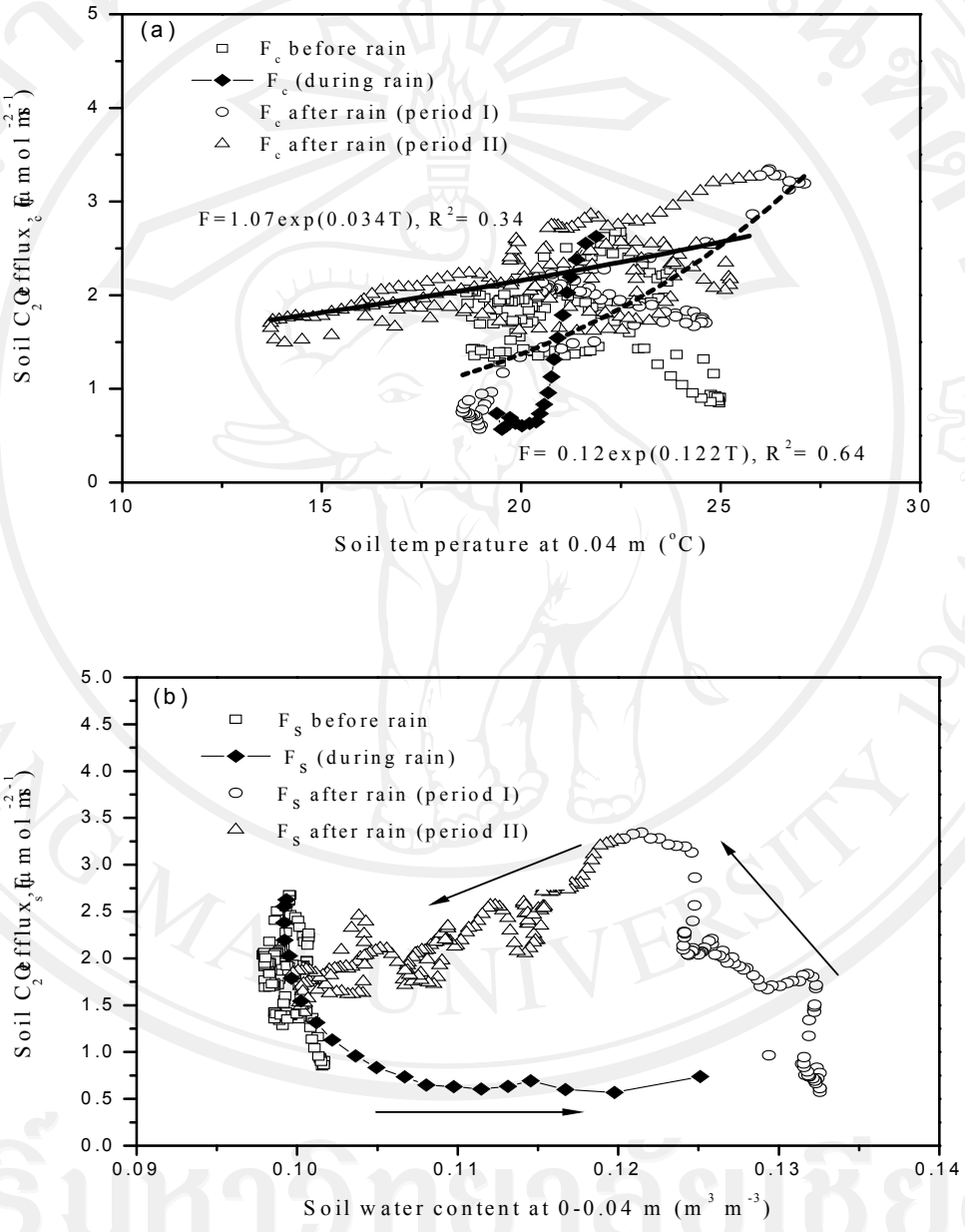

Figure 2.4 Relationships between soil CO_2 efflux and soil temperature (a) and soil water content (b) as influenced by rainfall event in the untrenched plot. Arrows indicate increasing time of day.

ลิขสิทธิ์มหาวิทยาลัยเชียงใหม่
Copyright© by Chiang Mai University
All rights reserved

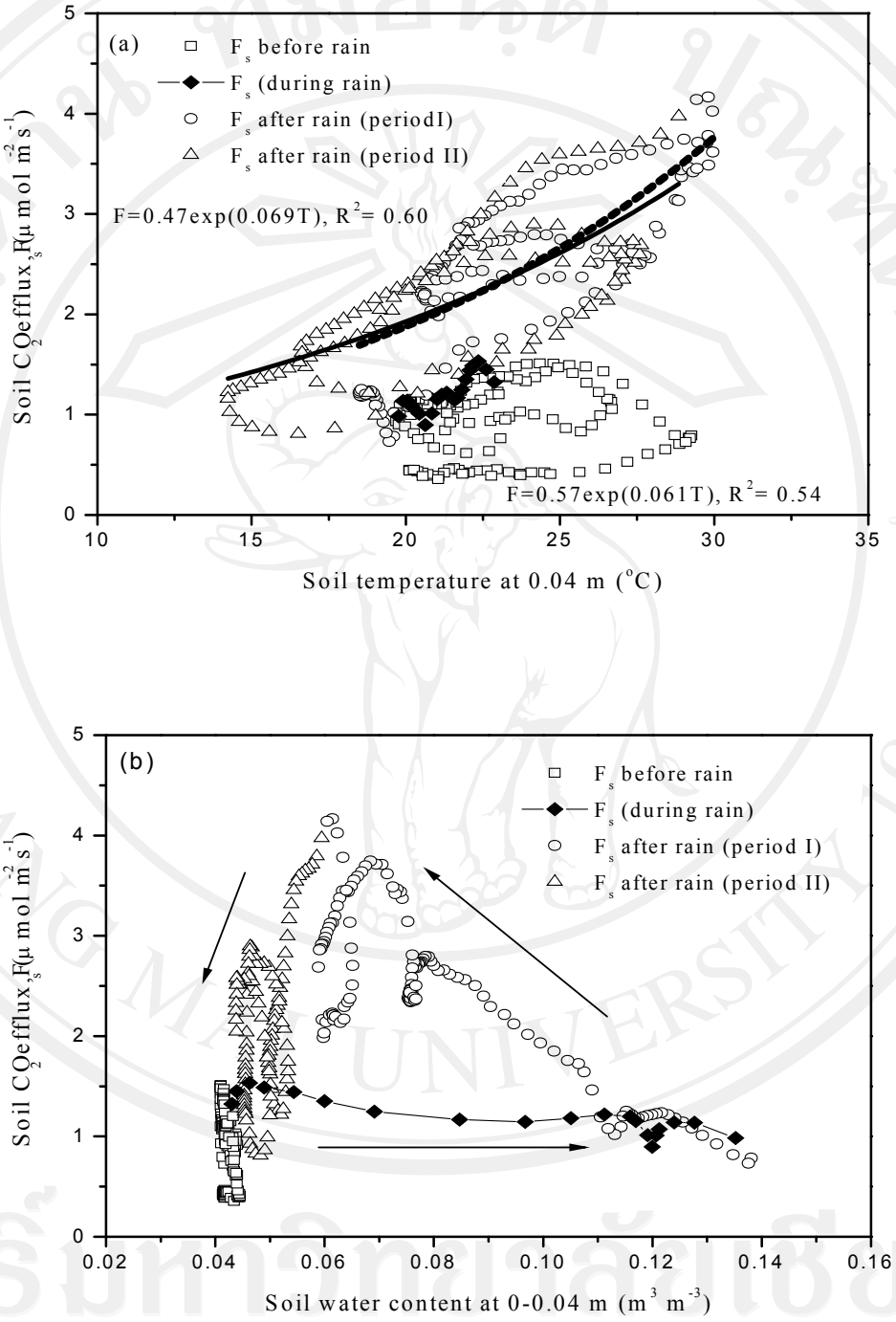

Figure 2.5 Relationships between soil CO_2 efflux and soil temperature (a) and soil water content (b) as influenced by rainfall event in the trenched plot. Arrows indicate increasing time of day.

ลิขสิทธิ์มหาวิทยาลัยเชียงใหม่
Copyright© by Chiang Mai University
All rights reserved

In addition, a new model was applied to simulate the response of soil CO_2 efflux caused by rainfall. Equation (7) describes how soil CO_2 efflux (F, μmol $m^{-2}s^{-1}$) changes with time (t, day) after rainfall, with t = 0 as the day when rainfall stops.

$$F = b_0 + b_1(\frac{t}{\tau})^2 e^{\frac{-t}{\tau}} \quad (7)$$

where F is the soil CO_2 efflux after rainfall (μmol $m^{-2}s^{-1}$), b_0 is the base respiration, or soil CO_2 efflux on the day when rainfall stops (μmol $m^{-2}s^{-1}$), b_1 is a coefficient that determines the maximal enchantment of soil CO_2 efflux after rainfall, and τ is a coefficient that indicates the dynamic time constant, which determines how long it takes for soil CO_2 efflux to decline to 1/e (e is the base for natural log) of its peak value(day).

The dynamic pattern of soil CO_2 efflux in response to rainfall in both fields (Fig 2.6) was best described by equation (7) with R^2 = 0.68 - 0.96 (Table 2.1). The maximal enhancement of soil CO_2 efflux to rainfall (b_1) and the dynamic time constant (τ) differed between the untrenched and trenched plots. Table 2.1 shows the coefficient b_1 was higher and the coefficient τ was lower in the trenched plot than in the untrenched plot. This indicates that soil CO_2 efflux at the trenched plot greatly increased after rainfall before it reached the peak and faster decreased after it reached the peak in response to rainfall than that of the untrenched plot. This pattern was similar with that pattern of soil water content change (Fig. 2.7). Soil water content in the trenched plot greatly increased after rainfall and faster decreased after it reached the peak in response to rainfall than that of the untrenched plot.

ลิขสิทธิ์มหาวิทยาลัยเชียงใหม่
Copyright© by Chiang Mai University
All rights reserved

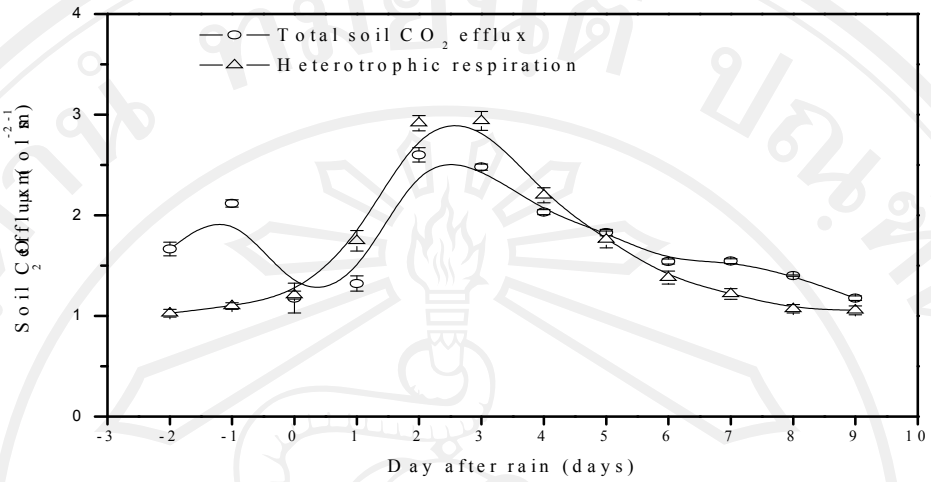

Figure 2.6 Total soil CO_2 efflux and heterotrophic respiration before, and 9-days period following a 7.8 mm rainfall event on DOY 90. Shown are mean and standard errors for 24 hr period. The day -1 represents 24 hr before the rainfall and the day 1 represents 24 hr after rainfall.

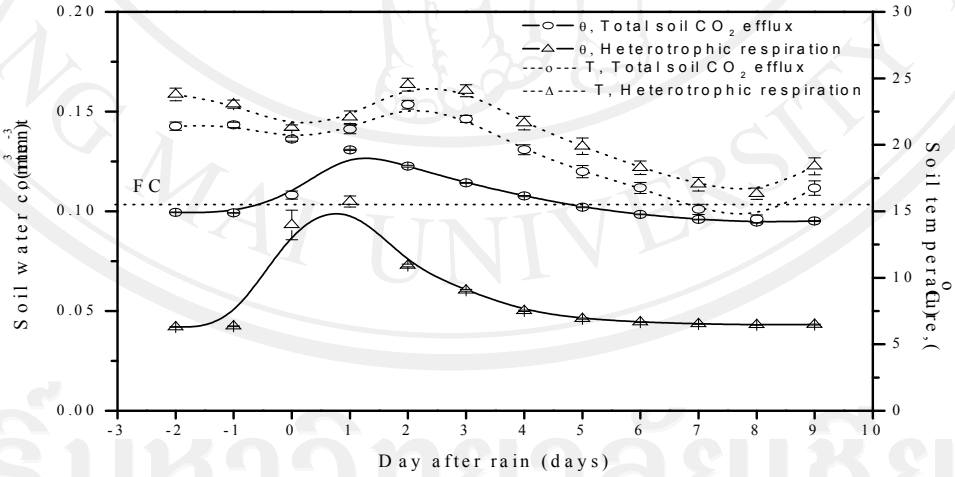

Figure 2.7 Soil volumetric water content (θ) at 0-0.04 m depth (FC, field capacity) and soil temperature (T) at 0.04 m depth in the untrenched (total soil CO_2 efflux) and trenched plots (heterotrophic respiration). The day -1 represents 24 hr before the rainfall and the day 1 represents 24 hr after rainfall.

ลิขสิทธิ์มหาวิทยาลัยเชียงใหม่
Copyright© by Chiang Mai University
All rights reserved

Table 2.1 Parameters of the exponential decay model of Equation 7 in wheat field. Abbreviations: b_0 is soil CO_2 efflux on the day when rainfall stops ($\mu molm^{-2}s^{-1}$); b_1 is a coefficient that determines the maximal enchantment of soil CO_2 efflux after rainfall; τ is a coefficient that indicates the dynamic time constant (day); and Decrease/Increase (%) is decrease/increase in soil CO_2 efflux due to rainfall event.

Plot	b_0	b_1	τ	R^2	Decrease (%)	Increase (%)
Untrenched	1.26	2.03	1.25	0.68	37.77	37.47
Trenched	0.90	3.62	1.17	0.96	13.62	176.3

Effect of soil temperature and soil water content on soil CO_2 flux

Under field condition, soil temperature and soil water content exhibited amplitude with respective influences on soil CO_2 efflux. The non-regression model was designed to describe the relationship between daily soil CO_2 flux and the environmental factors (soil temperature and soil water content).

The soil CO_2 efflux has a strong correlation with soil temperature. An exponential increase in soil CO_2 efflux with increasing soil temperature was observed in both plots. An exponential equation provided the best fit with highest correlation found with soil temperature at 0.08 m depth in both plots. The relationship between daily soil CO_2 efflux and soil temperature differed between the untrenched and trenched plots. The relationship between soil CO_2 efflux and soil temperature was found to have a relatively strong dependence on volumetric soil water content in the

ลิขสิทธิ์มหาวิทยาลัยเชียงใหม่
Copyright© by Chiang Mai University
All rights reserved

untrenched plot (Fig. 2.8). Soil CO_2 efflux in the untrenched plot had a greater response on soil temperature with soil water content more than 0.16 m $^3m^{-3}$ with R^2 = 0.59 (Fig. 2.8). Soil CO_2 efflux in trenched plot responded soil temperature in two groups of DOY 67-90 and DOY 91-116, with soil CO_2 efflux in the second group of period higher than in the first group at similar soil temperature (Fig. 2.9).

The Q_{10} value is used to describe the temperature dependence of soil temperature. The results showed that temperature sensitivity of daily soil CO_2 effluxes varied among different plots. Temperature sensitivity of soil CO_2 efflux in the untrenched plot was influenced by different soil water content. The Q_{10} values were low when 0.13 < soil water content < 0.16 m^3m^{-3} and high at soil water content > 0.16 m^3m^{-3}. Additionally, the Q_{10} value in the trenched plot during DOY 67-90 was lower than during DOY 91-116.

The influence of soil water content on soil CO_2 efflux was more complex than that of temperature. The relationship between soil CO_2 efflux and soil water content is described by the quadratic function. The results showed that with soil water content increasing, daily soil CO_2 efflux increased when the soil water content was below 0.150 and 0.17 m^3 m^{-3} and decreased when the soil water content was great than 0.150 and 0.17 m^3 m^{-3} or 0.105 m^3 m^{-3} in the untrenched and trench plots, respectively (Fig. 2.10a and b). The outliers around soil water content of 0.14 m^3m^{-3} in the untrenched plot with extremely high values of soil CO_2 efflux were probably due to rainfall effect. In the trenched plot, soil water content did not predict soil CO_2 flux well during DOY 67-90. However, the 44% of variation in daily soil CO_2 efflux during DOY 91-116 was explained by Equation (5).

ลิขสิทธิ์มหาวิทยาลัยเชียงใหม่
Copyright© by Chiang Mai University
All rights reserved

Soil CO_2 efflux in the untrenched plot exhibited increasing with soil water content and gave higher correlation than soil temperature. This meant that soil temperature was not the major factors that influenced soil CO_2 efflux. At this point, it is quite obvious that both soil water content and soil temperature controlled and soil water content might be the major influencing parameter on the soil CO_2 efflux in the untrenched plot. While, soil CO_2 efflux in the trenched plot exhibited increasing with soil temperature and gave higher correlation than soil water content. Soil temperature might be the major influencing parameter on the soil CO_2 efflux in the trenched plot.

ลิขสิทธิ์มหาวิทยาลัยเชียงใหม่
Copyright© by Chiang Mai University
All rights reserved

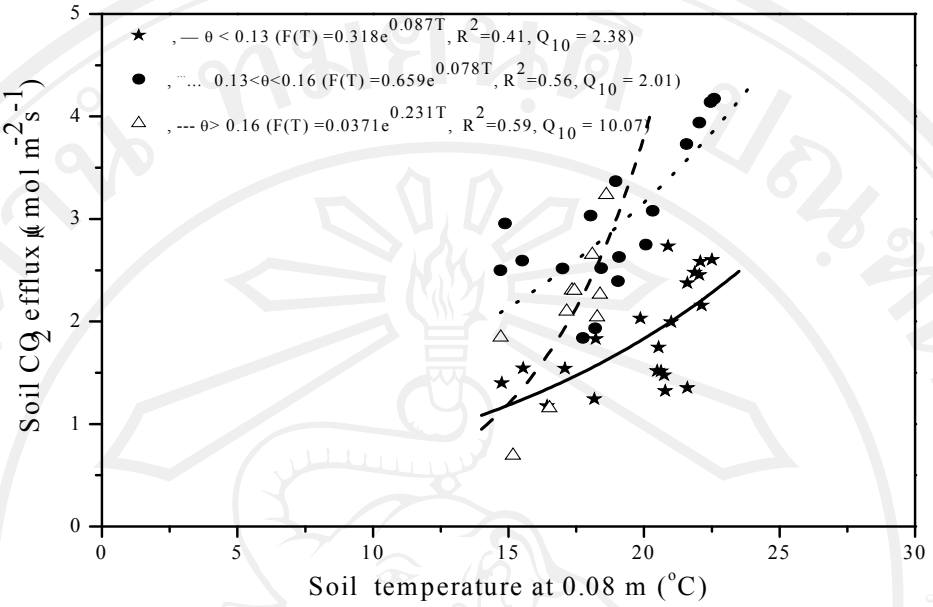

Figure 2.8 The relationship between daily mean soil CO_2 efflux and soil temperature at 0.08 m depth in the untrenched plot. Lines show fit to Equation 3 for each soil water content range.

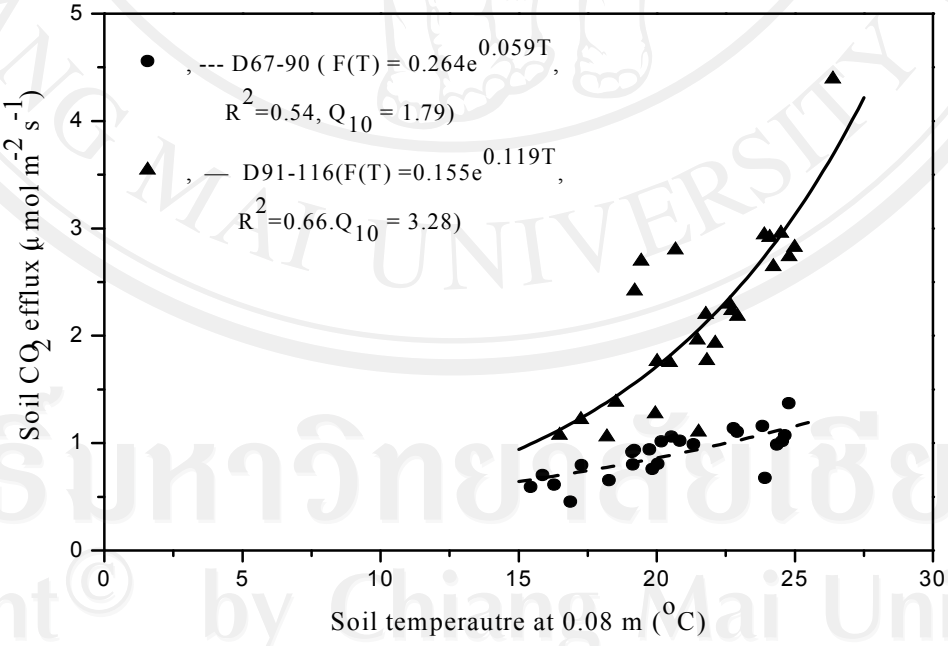

Figure 2.9 The relationship between daily mean soil CO_2 efflux and soil temperature at 0.08 m depth in the trenched plot. Lines show fit to Equation 3 for each period.

ลิขสิทธิ์มหาวิทยาลัยเชียงใหม่
Copyright© by Chiang Mai University
All rights reserved

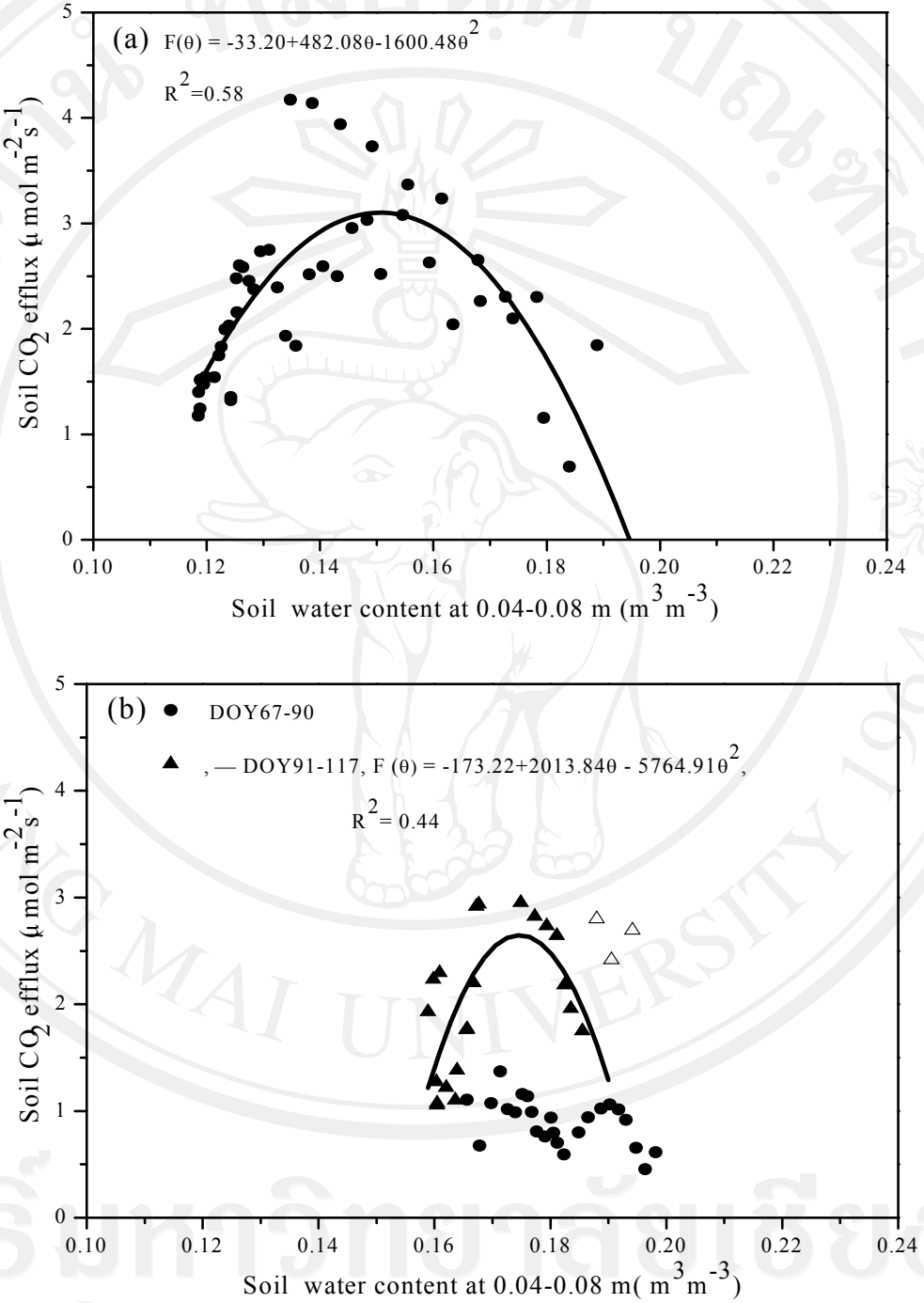

Figure 2.10 The relationship between daily mean soil CO_2 efflux and soil water content at 0.04-0.08 m at the untrenched (a) and trenched plots (b). Lines show fit to Equation 5.

ลิขสิทธิ์มหาวิทยาลัยเชียงใหม่
Copyright© by Chiang Mai University
All rights reserved

Statistical models of soil CO_2 efflux and related environmental factors

Three empirical models were selected and fitting against daily mean soil CO_2 efflux, soil temperature and soil water content data. A daily data set of 48 observations from the untrenched plot and 48 observations from the trenched plot were used Table 2.2 summarizes the coefficients of determination and best single- and multiple-factor models obtained from evaluating the influences of the soil temperature and soil water content factors on the soil CO_2 efflux. For the untrenched plot, single regression with soil water content, $F(\theta)$, gave batter results than single regression with temperature. Soil water content explained 58% of the seasonal changes of soil CO_2 efflux using quadratic function. For the trenched plot, bivariate model including soil temperature and water content function, $F(T,\theta)$, can explained variation of soil CO_2 efflux batter than univariate models with soil temperature and water content.

The simultaneously measured soil CO_2 efflux data was used to compare with estimated soil CO_2 efflux data. Three empirical models that predicted soil CO_2 efflux were selected and fitted against measured soil CO_2 efflux data (Fig. 2.11a, b and c). The results show that the estimated soil CO_2 efflux data was correlated well with measured soil CO_2 efflux data. About 76% and 87% of measured soil CO_2 efflux was explained by the $F(\theta)$ and $F(T,\theta)$ equation in the untrenched and trenched plots, respectively. But for soil water content plots, estimated soil CO_2 efflux in the untrenched plot using quadratic function, $F(\theta)$ trend to slightly underestimate soil CO_2 efflux. Conversely, estimated soil CO_2 efflux in the trenched plot using bivariate function, $F(T,\theta)$ trend to slightly underestimate soil CO_2 efflux during DOY 91-116.

ลิขสิทธิ์มหาวิทยาลัยเชียงใหม่
Copyright© by Chiang Mai University
All rights reserved

Table 2.2 Models of soil CO_2 efflux from the untrenched and trenched plots (F, μmol m^{-2} s^{-1}) against soil temperature (T, °C) at 0.08 m depth and volumetric soil water content (θ, m^3m^{-3}) at 0.04-0.08 m depth.*

Equation	a*	b*	c*	d*	R^2	Q_{10}
Untrenched plot						
1. Soil Temperature						
$\theta < 0.13$	0.32	0.08	-	-	0.41	2.38
$0.13 < \theta < 0.16$	0.66	0.07	-	-	0.55	2.01
$\theta > 0.16$	0.37	0.23	-	-	0.59	9.97
2. Soil water content						
DOY 67-116	-33.20	482.08	-1,600.48	-	0.58	-
3. Soil temperature and water content						
DOY 67-116	-11.19	0.06	140.86	-444.18	0.53	-
Trenched plot						
1. Soil temperature	0.26	0.06	-	-	0.54	1.79
DOY 67-90	0.15	0.11	-	-	0.65	3.28
DOY91-116						
2. Soil water content	-	-	-	-	-	
DOY 67-90	-173.22	2,013.84	-5,764.91	-	0.44	
DOY91-116						
3. Soil temperature and soil water content	-37.44	0.08	387.41	-1,049.83	0.65	
DOY 67-90	-20.01	0.12	208.04	-594.30	0.83	
DOY91-116						

*a, b, c, d are significant coefficients ($P < 0.05$). R^2 stand for determination coefficient. All models are significant ($P < 0.05$).

ลิขสิทธิ์มหาวิทยาลัยเชียงใหม่
Copyright© by Chiang Mai University
All rights reserved

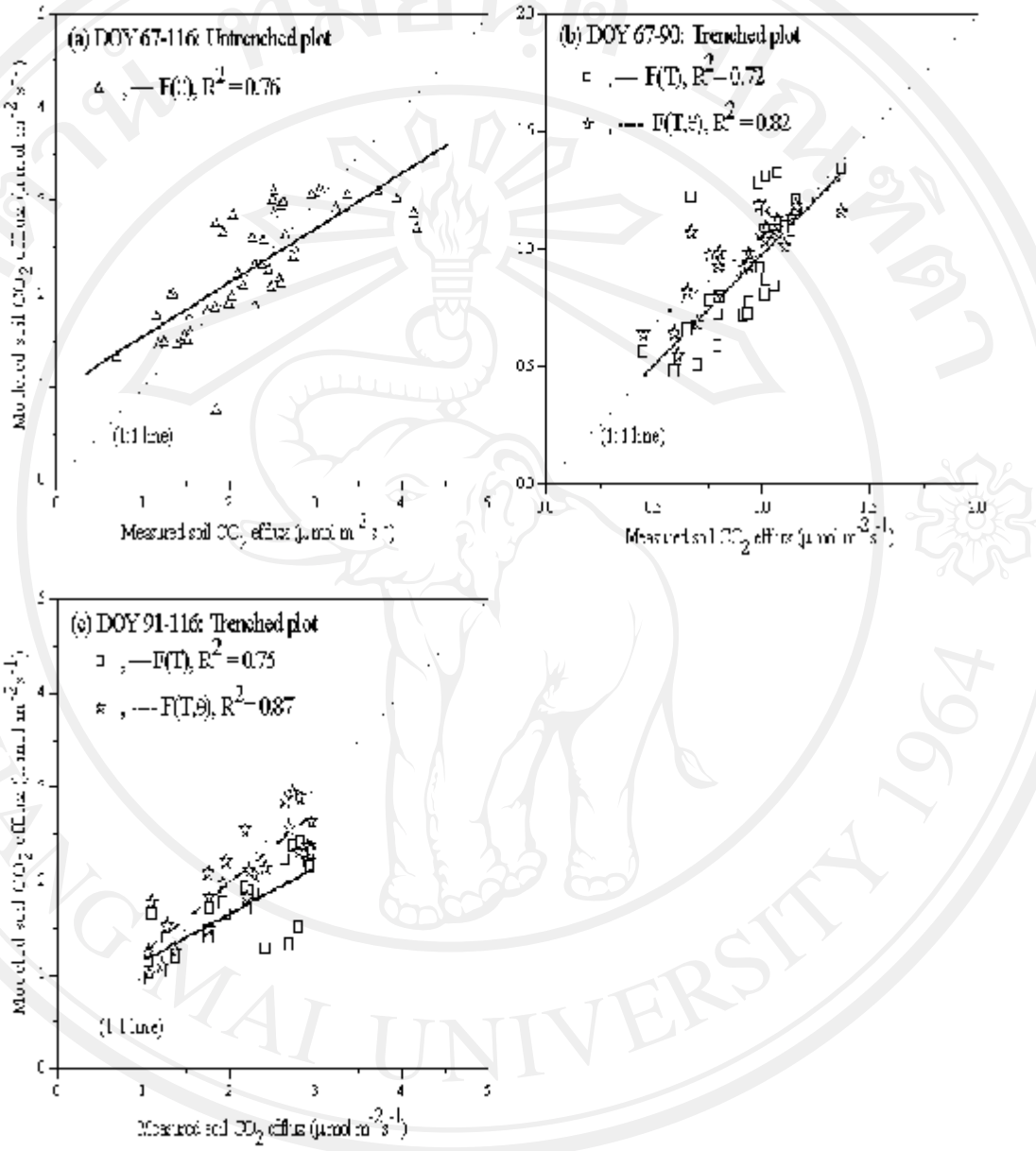

Figure 2.11 Comparison of measured and modeled soil CO_2 efflux in the untrenched and trenched plots: function of soil water content, F(θ) in the untrenched plot (a) and function of soil temperature, F(T) and function of soil temperature and soil water content, F (T,θ) in the trenched plot (b,c). The lines are y = a + bx.

ลิขสิทธิ์มหาวิทยาลัยเชียงใหม่
Copyright© by Chiang Mai University
All rights reserved

DISCUSSION

Mechanisms of soil CO_2 efflux during and following rainfall

Many studies have explained mechanisms that controlled soil CO_2 efflux during and after rainfall in different conditions including (1) degassing or displacement of soil air by rainfall and inhibition of gaseous movement in water saturated soil, (2) translocation, quality and quantity of substrate, and (3) production of CO_2 in the soil due to enhanced microbial activity (Lee *et al.,* 2002; Lee *et al.,* 2004; Xu *et al.,* 2004). In half-hour fluxes, soil CO_2 concentration, [CO_2] at 0.04 and 0.08 m depths increased during and after rainfall, but the flux decreased immediately. This reduction in soil CO_2 efflux was associated with the lack of a continuous air-filled pore space pathway to the atmosphere. The main cause for this could be the reduction of the soil air- filled pore space resulting in reduced gaseous diffusivities. As precipitation progressively saturates the soil surface, gas exchange between the soil and the atmosphere is reduced accordingly slowing down the diffusion of CO_2 out of the soil and leading to a rapid storage of [CO_2] in the soil profile. Consequently, this does not lead to an increase in soil CO_2 efflux. These findings are similar to those from Smart and Peñuelas (2005); Jassal *et al.* (2005) and Chen *et al.* (2005) who found decreased soil CO_2 efflux immediately following rainfall due to reduction of soil diffusivity. There is some evidence that the lower soil CO_2 efflux during rainfall may be caused by the dissolution of soil air CO_2 into the filtrating water (Rochette *et al.,* 1991) and the restriction of the soil macroporosity (Ball *et al.,* 1999). Myklebust *et al.* (2008) reported that water may combine with CO_2 and Ca, and then form $CaCO_3$. Amount of CO_2 may go to $CaCO_3$ formation than to the atmosphere.

ลิขสิทธิ์มหาวิทยาลัยเชียงใหม่
Copyright© by Chiang Mai University
All rights reserved

Quite possibly that wheat root contributed significantly to CO_2 production in soil that is characterized by a fast increase and a higher peak of [CO_2] during and after a rain event in the untrenched soil (Fig. 2.2). The higher [CO_2] found in the 0.04 and 0.08 m depths soil layers is likely to be a result from higher rate of CO_2 production or a reduction in rate of diffusion or both. Sotta *et al.* (2004) and Tang *et al.* (2005) reported that the high CO_2 concentration in the top soil after rainfall in not only result from a higher rate of CO_2 production but a result of a reduction in the rate of diffusion of CO_2 with in the top soil pore space. However, soil CO_2 efflux in the untrenched plot was lower than in the trenched plot due to a small CO_2 concentration gradient and change in diffusivity. This suggests that most of CO_2 production in wheat soil located within and perhaps surrounding the 0.04 to 0.08 m depth.

Many studies report an increase in soil CO_2 efflux for a few days following a rainfall event due to enhanced microbial activity with increased soil water content (Xu *et al.,* 2004; Lee *et al.,* 2004; Huxman *et al.,* 2004). In this current study, it is likely that the fast increase in [CO_2] and soil CO_2 efflux after rainfall in both plots is due mainly to an increase in soil diffusion corresponding with decrease in soil water content (Fig. 2.4b and 2.5b) or CO_2 produced by microbes. When water was redistributed and a decrease in surface water content and then displaced by the soil air, gas diffusion increased in the period in which soil water content decreased after rainfall. It is likely that rapid soil drying caused by high evaporation rates of surface moisture over soil surface, in parallel with a diurnal increase in soil temperature, lead to rapid increases in CO_2 diffusion and simulates microbial activity which trends to highly enhance soil CO_2 efflux.

ลิขสิทธิ์มหาวิทยาลัยเชียงใหม่
Copyright© by Chiang Mai University
All rights reserved

One possible hypothesis is that organic matter accumulated in the soil becomes available for decomposition by microbial activity. This newly available C substrate leads to an increase in microbial population and activity, resulting in a rapid increase in soil CO_2 efflux after rainfall (Murphy *et al.,* 1998). However, the agricultural soil in this experiment differs from forest and grassland soils with regards to the absence of litter layer and soil texture. The results suggest that a small rainfall event (7.8mm) would stimulate microbial activity at the soil surface to break down soil organic matter. The presence of large substrates available for microbial activity dominates the response in these data.

Response of total soil CO_2 efflux in the untrenched plot and heterotrophic respiration in trenched plot to rainfall

Rainfall stimulated soil CO_2 efflux in both plots. In response to rainfall, daily soil CO_2 efflux decreased during the rainfall. A few days later, soil CO_2 efflux increased, reached a peak and then declined to the pre-rain value (Fig 2.6). The dynamic pattern of soil CO_2 efflux to natural rainfall in this study is similar to the response to water addition and natural rainfall events in forest and grassland soils (Liu *et al.,* 2002; Tang *et al.,* 2005; Smart and Peñuelas, 2005), but exhibited different response times. The previous studies showed that the time taken for soil CO_2 efflux to return to pre-rainfall values was about 30 days after a natural 18-mm rainfall event in Mediterranean soils (Jarvis *et al.,* 2007) and 7 days period following water addition in greenhouse experiment (Smart and Peñuelas, 2005). In this study, the root and microbial respirations in both plots took shorter response times than the response in forest soil due to the activation of root activity of fast-growth crop and available

ลิขสิทธิ์มหาวิทยาลัยเชียงใหม่
Copyright© by Chiang Mai University
All rights reserved

subtracts for microbial decomposition. The observations suggested that the impact of rainfall events on soil CO_2 efflux from agricultural soil is relatively short in duration. However, rainfall events stimulated soil CO_2 efflux in both plots. The impact of rainfall events might contribute to a relative small fraction of the total CO_2 released to atmosphere and reduce carbon mineralization in soil, depending on frequency of rainfall event.

Many researchers (Davidson *et al.,* 2000; Liu *et al.,* 2002; Xu *et al.,* 2004; Tang *et al.,* 2005) used exponential model to predict the response in soil CO_2 to rainfall. They computed the dynamic time constant (τ) to quantify the time when soil CO_2 efflux decreases after the rainfall event. In this study, the Equation 7 was calculated and used to determine the dynamic time constant. In this results, the shape of the response was described well by an exponential decay, the model could explain very well (R^2 = 0.60-0.96). This equation can be highly useful for modeling studies to estimated annual carbon budget that account for dynamic variation in soil CO_2 efflux between rainfall events. Additionally, for the same amount of rainfall, the enhancement of soil CO_2 efflux after rainfall (b1) in the trenched plot was faster than for the untrenched plot. This is probably due to the increase in microbial activity and population for the changes of soil water content in the soil surface layer in the trenched plot. Murphy *et al.* (1998) reported that microbial activity increased (within 4 hr) after wetting dry soil. This may also be attributed to the increased availability of substrates such as soil organic matter and microbial death. Those substrates become more available for use by the surviving microbial populations when the soil is re-wet. One possibility is that organic matter accumulates in the soil during dry periods with low decomposition in the trenched plot. After rewetting by rainfall, the microbe

ลิขสิทธิ์มหาวิทยาลัยเชียงใหม่
Copyright© by Chiang Mai University
All rights reserved

population recovers and starts utilizing fresh dead organic matter in the soil. The surviving microbial can utilize carbon substrates immediately when rainfall occurs. Moreover, the increase in soil water content when soil was dry in the trenched plot may make the physical environment favorable to microbial activity. The higher peak of soil CO_2 efflux in the trenched plot might have caused as the reason earlier.

Otherwise, the time constant (τ) of soil CO_2 efflux at the untrenched plot was longer than for the trenched plot because of root activity and shading by canopy reducing the evaporation rate of soil. Thus, soil under canopy dries out slowly, soil water content in the untrenched plot must have remained high, resulting in an increase in root activity. Soil CO_2 flux was reduced gradually, causing a long soil CO_2 efflux. This result indicated that the decrease in soil CO_2 efflux after rainfall may depend on amount of soil water content, transpiration and evaporation.

Response of soil CO_2 efflux to soil temperature and soil water content

The seasonal variation in soil CO_2 efflux in a wheat field was explained by changes both in soil temperature and soil water content. The variation in soil CO_2 efflux are generally predicted by soil temperature (Lloy and Taylor, 1994; Davidson, 1998; Xu and Qi, 2001), soil water content alone (Keith *et al.,* 1997; Epron *et al.,* 2004), or both (Bunnell *et al.,* 1977; Mielnick and Dugas, 2002; Tang *et al.,* 2005). In many research studies, soil temperature was noted to be strong and positive predictor of soil CO_2 efflux of many croplands under different conditions (Lee and Jose, 2003; Shi *et al.,* 2006; Han *et al.,* 2006; Qi *et al.,* 2007). This study found both soil temperature and soil water content varied markedly with period and soil CO_2 efflux varied on both soil temperature and soil water content.

ลิขสิทธิ์มหาวิทยาลัยเชียงใหม่
Copyright© by Chiang Mai University
All rights reserved

The high correlation between soil CO_2 efflux and soil water content could explain well the seasonal variation in soil CO_2 efflux in the untrenched plot. Soil water content could explain 58% variations of soil CO_2 efflux, whereas significant exponential relationships between soil temperature and soil CO_2 efflux were found under differences in range of soil water content. Soil temperature accounted 41-59% variations of soil CO_2 efflux. Additionally, sensitivity of soil CO_2 efflux to temperature is commonly expressed by the coefficient Q_{10}. Davidson *et al.* (2006) reported that the Q_{10} varies with soil temperature, soil water content and the seasons. The results showed that the Q_{10} value in the untrenched plot varied with soil water content, indicating that the apparent temperature sensitivity of soil CO_2 efflux was influenced by soil water content. Therefore, soil water content was a major limiting factor soil CO_2 efflux in the untrenched plot.

On the other hand, soil temperature and water content were the limiting factor for carbon decomposition and microbial activity in the trenched plot without roots. Soil temperature alone could explain 54% and 66% variations of soil CO_2 efflux during period of DOY 67-90 and DOY 91-116, respectively, whereas soil water content accounted 44% variations of soil CO_2 efflux during the second period. While both soil temperature and water content could explain 65% and 85% variations of soil CO_2 efflux during period of DOY 67-90 and DOY 91-116, respectively. The Q_{10} during first period was lower than the second period and this different was attributed to limitation imposed by the drought condition on decomposition by microbial activity during the first period. Previous study have demonstrated that Q_{10} can also differ seasonally, related to the distribution of rainfall and soil water content (Rey *et al.,* 2005). Although the difference in soil temperature and soil water content in

ลิขสิทธิ์มหาวิทยาลัยเชียงใหม่
Copyright© by Chiang Mai University
All rights reserved

both periods were very small. Soil water content during the second period was high fluctuated by rainfall throughout the period. These data are likely to be indicated that some other than temperature such as rainfall might influence soil CO_2 efflux during the second period and its temperature sensitivity.

In this study, soil temperature and soil water content exerted control over the seasonal variation in soil CO_2 efflux. The soil CO_2 efflux in the untrenched and trenched plots might also respond differently to soil temperature and soil water content. The soil CO_2 efflux in the untrenched plot with roots was higher controlled by soil water content than soil temperature. While, the soil CO_2 efflux in the trenched plot without roots was controlled by both soil temperature and soil water content but soil temperature seem to be the most influenced factor. Base on multivariate regression analysis (Table 2.2), the interacted exponential model better fitted to observed data and also explained approximately of 83% of the variation in daily soil respiration in the trenched plot.

It is clear that soil CO_2 efflux responds positive to soil temperature. Increasing temperatures in the trenched plot may promote microbial activity and increase microbial decomposition rate, thus simulating soil CO_2 efflux. Similarly, increasing temperature in the untrenched plot may influence the photosynthesis of the plant, photosynthates translocated from the above ground part of the plant to the soil and root exudates, thus simulating soil CO_2 efflux from root (Curiel-Yuste *et al.,* 2004).

In addition, soil water content had both negative and positive direction effects on soil CO_2 efflux, depending on range of soil water content. The critical values of soil water content in the untrenched and trenched plots were 0.150, and 0.180 m^3 m^{-3}, respectively. Soil CO_2 efflux increased with increasing in soil water content until a

ลิขสิทธิ์มหาวิทยาลัยเชียงใหม่
Copyright© by Chiang Mai University
All rights reserved

critical value. This soil water content may promote microbial decompositions and root activity. While soil CO_2 efflux decreased with increasing in soil water content above a critical value. This soil water content may reduce microbial activity by limiting the flux of oxygen into soil of microbial activity. This results supported by Raich and Potter (1995) and Reichstein *et al.* (2003) that when soil are dry, metabolic activity increases with increasing soil water content; when soil are above soil capacity and toward saturation, oxygen deficiencies inhibit aerobic microbial activity.

Effects of plot trenching on measurements of heterotrophic respiration and environmental factors

Heterotrophic respiration in the 3m x 3m trenched plot may be underestimated because this trenched method severed the food to microbe such as root exudates and root residuals within the trenched plot, resulting in reduced microbial activities that convert soil organic matter derived from dead roots into CO_2. Generally, root can also affect soil microbial growth and activity by altering the physical and chemical environment (Kuzyakov and Cheng, 2001). Therefore, absence of root and root residuals in the trenched plot might reduce microbial activity, thereby reducing heterotrophic respiration. In addition, the difference in microbial population between the trenched and untrenched plots should be considered. Several authors have shown that microbial biomass and root residual biomass in the trenched plot also affected microbial decomposition activity (Jiang *et al.,* 2005; Ngao *et al.,* 2007).

This result showed that trenching modified soil environmental conditions. Plot trenching overall tended to increase both soil temperature and water content. There was significant difference in soil temperature and soil water content between

ลิขสิทธิ์มหาวิทยาลัยเชียงใหม่
Copyright© by Chiang Mai University
All rights reserved

the untrenched and trenched plots. The open area of the trenched plot had higher soil temperature and soil water content than the untrenched plot. There was no shading of canopy but there was the influence on direct solar radiation that would lead to increases in high diurnal variation in soil temperature within the trenched plot, resulting in a significant difference in daily soil temperature between the untrenched and trenched plots. Trenching overall increased soil water content probably because of the elimination of plant water uptake and plant transpiration. Plants in the untrenched plot absorb soil water through their roots and evaporate through stomata, causing more reduction in soil water content. Thus, because of the absence of plant in the trenched plot, soil water content might still remain high. The changed soil temperature by trenching exerted a strong impact on soil respiration measurements in the trenched plot than did the changed soil water content. This result illustrates that in order to the estimate and compare heterotrophic respiration, environmental changes caused by plot trenching should also be taken into account. This trench method in this experiment does not provide a quantitative estimate of contribution from root respiration to total soil CO_2 efflux, but much can be gained by examining such temporal variation.

ลิขสิทธิ์มหาวิทยาลัยเชียงใหม่
Copyright© by Chiang Mai University
All rights reserved

Sub-Experiment 2: Net ecosystem exchange in a winter wheat field in relation to biophysical properties and rainfall

INTRODUCTION

Changes in the global climate system due to increased levels of CO_2 and other greenhouse gases are predicted to significantly impact the Earth's terrestrial ecosystems. The increased atmospheric CO_2 concentration is most likely responsible for the observed increase of both mean air and soil temperatures, and alters rainfall pattern (IPCC, 2007). Terrestrial ecosystems are coupled to the climate system through both the carbon cycle and the hydrological cycle. Climate change affects carbon storage in these ecosystems since both photosynthetic uptake of carbon and loss of carbon through respiration of plants and soils are dependent on temperature, moisture and radiation. The net carbon uptake is not fully understood and it is thus difficult to make reliable projections of how terrestrial ecosystems will respond to the ongoing climate change. It is therefore of great importance to increase the knowledge of the biogeophysical and biogeochemical processes in these ecosystems.

Eddy covariance technique is one of the best micrometeorological methods for estimating the CO_2, water, and energy exchange between the atmosphere and terrestrial ecosystems. In recent years, many studies have used eddy covariance techniques to measure net ecosystem exchange of CO_2 (NEE), and the resultant NEE data provide valuable information related to photosynthesis period, gross primary production (GPP) and respiration of ecosystems (Baldocchi, *et al.,* 2002; Tenhunen *et al.,* 2002). Analysis of the continuous NEE observations provides information

ลิขสิทธิ์มหาวิทยาลัยเชียงใหม่
Copyright© by Chiang Mai University
All rights reserved

about the interactions among ecosystem phenological stage, variation in physiological characteristics and the associated driving environmental variables.

Exchange of CO_2 between terrestrial ecosystems and the atmosphere is controlled by the balance between CO_2 uptake during photosynthesis (gross primary production, GPP) and CO_2 emission via plant and soil respiration (ecosystem respiration). Photosynthetic uptake and respiratory release are separated processes, with different responses to environmental change. Gross primary production is dependents in temperature, radiation and moisture during the growing season when temperature is adequate for growth (Carrara *et al.,* 2004; Suyker *et al.,* 2005; Jaksic *et al.,* 2006), whereas ecosystem respiration is mainly regulated on temperature and moisture (Xu *et al.,* 2004; Xu and Baldocchi, 2004; Flanagan and Johnson, 2005). Although recent studies also suggested a tight coupling between those processes, light, temperature, and moisture are out of phase over the course of the year. The photosynthetic uptake and respiratory release may have dissimilar periods of activity.

Since the wheat ecosystems are usually grown under rainfed condition, water availability is highly unpredictable over the course of the year. Wheat growth systems are very complex and dynamic in there interactions between living organisms and the environment. Rainfall variability and subsequent dry periods may differentially affect the activity of plants and soil microbes, combining to influence the ecosystem carbon exchange. Therefore, it is essential to investigate separately environmental parameters affect the plant photosynthesis and ecosystem respiration.

Net ecosystem exchange of CO_2 and its variation characteristics as well as the controlling environment factors were analyzed in this study by using eddy-covariance measurements. The objectives of this were to (1) to quantify the seasonal distribution

ลิขสิทธิ์มหาวิทยาลัยเชียงใหม่
Copyright© by Chiang Mai University
All rights reserved

of net CO_2 exchange in wheat during a growing season and (2) to examine how key environmental controls influence those carbon exchanges.

MATERIALS AND METHODS

The research was carried out at the University of Georgia's Southwest Georgia Research and Education Center in Plains, GA, USA during December 2006 to May 2007.

Eddy covariance flux measurement

The eddy-covariance technique was used to measure net ecosystem carbon exchange and the fluxes of water vapor and sensible heat. The eddy-covariance sensors were mounted at a height of 2.5 m above the ground. The tower placement in the field provides a fetch over a continuous crop with 400m to the north. The prevailing winds during the water are from the west to northwest. An open-path eddy-covariance system consisting of a sonic anemometer and a CO_2/H_2O gas analyzer were used to measure CO_2, sensible and latent heat above the canopy. Wind velocities and temperature were measured with a three-dimensional ultrasonic anemometer (CSAT-3, Campbell Scientific, Logan, UT). The CO_2 and H_2O concentrations were measured with an open path infrared gas analyzer (LI7500, Li-COR Inc., Lincoln, NE). The LI 7500 head were tilted 15South and 0.2 cm horizontally from the CSAT-3 head in order to avoid direct sunlight contamination in the optical path and to facilitate the draining of rain water from the lower lens surface. The eddy covariance technique applied here is based on the assumption that the flux of a given scalar

ลิขสิทธิ์มหาวิทยาลัยเชียงใหม่
Copyright© by Chiang Mai University
All rights reserved

parameter can be measured as an average of the covariance between the10-Hz fluctuations in the vertical wind speed and the 10-Hz fluctuations of the scalar parameters. All raw data were collected at a rate of 10-Hz by a datalogger (CR1000, Campbell. Scientific, Logan, UT) and saved for later reprocessing.

Supporting measurements

Along with the eddy-covariance technique, standard meteorology and soil parameters were measured continuously with an array of sensors, included net radiation (Model NR-LITE, Kipp and Zonen USA Inc., Bohemia, NY), rainfall (tipping-bucket raingauge,TE525, Campbell. Scientific, Logan, UT), relative humidity and temperature (CS500, Campbell. Scientific, Logan, UT). Soil heat flux was measured with two heat flux plates (HFT3, Campbell Scientific, Logan, UT): one within the plant row and the second in the inter-row space, installed at 0.08 m below the soil surface and were randomly placed within a few meters of the flux system. Soil thermocouples were placed at 0.02 and 0.08 m below the surface and above each soil heat flux plate to compute the storage component of the soil heat flux. Soil water content was measured by time-domain reflectometers (CS616, Campbell. Scientific, Logan, UT) to permit calculation of heat capacity. All data was recorded on datalogger (CR1000, Campbell. Scientific, Logan, UT), and then 30 min average data was stored.

Green leaf area index (GLAI) and aboveground biomass were estimated from destructive samples at 7 days intervals until physiological maturity. One meter linear row sections were destructively sample at approximately six different locations.

ลิขสิทธิ์มหาวิทยาลัยเชียงใหม่
Copyright© by Chiang Mai University
All rights reserved

Flux calculation

The 30-min mean CO_2 fluxes were calculated from the 10-Hz time series data. Before covariance calculation the time series were de-spiking and linearly detrended. The fluxes were three-dimensional coordinate rotations (Wilczak *et al.,* 2001) to align the sonic anemometer axis along the long-term streamlines and WPL-correction (Webb *et al.,* 1980). Following the sign convention in the atmospheric flux community, positive flux covariance represent net carbon gain by the atmosphere and loss from the ecosystem; conversely, negative values indicate a loss of carbon from the atmosphere and gain by the ecosystem. The flux data were rejected following these criteria (1) wind direction, (2) rainy days, and (3) clam conditions. For clam nighttime condition, CO_2 flux is often underestimate by the eddy covariance system. The nighttime net ecosystem exchange (NEE) was examined in relation to a wind friction velocity (*u**). It is assumed that the u* threshold is located where the flux starts to level off as u* increases (Falge *et al*., 2001). In this study, the u* threshold about 0.1 m/s was used. The fluxes measurements when *u** was smaller than the threshold were removed from the dataset to minimize problems related to insufficient turbulent mixing (Fig. 2.12).

Data screening and Gap filling

To separate NEE into photosynthetic and respiration fluxes, NEE were divided into daytime and nighttime periods to develop non-linear regressions for evaluating environmental effects on NEE. All data records with solar altitude less than 0 were used to estimate ecosystem respiration (Re).

ลิขสิทธิ์มหาวิทยาลัยเชียงใหม่
Copyright© by Chiang Mai University
All rights reserved

An eddy covariance system can rarely produce good quality data for 24 h a day. Several reasons exist for the occurrences of gaps (Falge *et al.,* 2001). Gap in half- hourly data were filled with empirical regressions for respiration and net CO_2 uptake derived for two weekly intervals. When daytime half-hourly values in wheat dataset were missing, the CO_2 flux was estimated as a hyperbolic function of income radiation. To minimize problems related to insufficient turbulent mixing at night, the CO_2 flux when u* was smaller than the threshold was estimates as an exponential function of temperature.

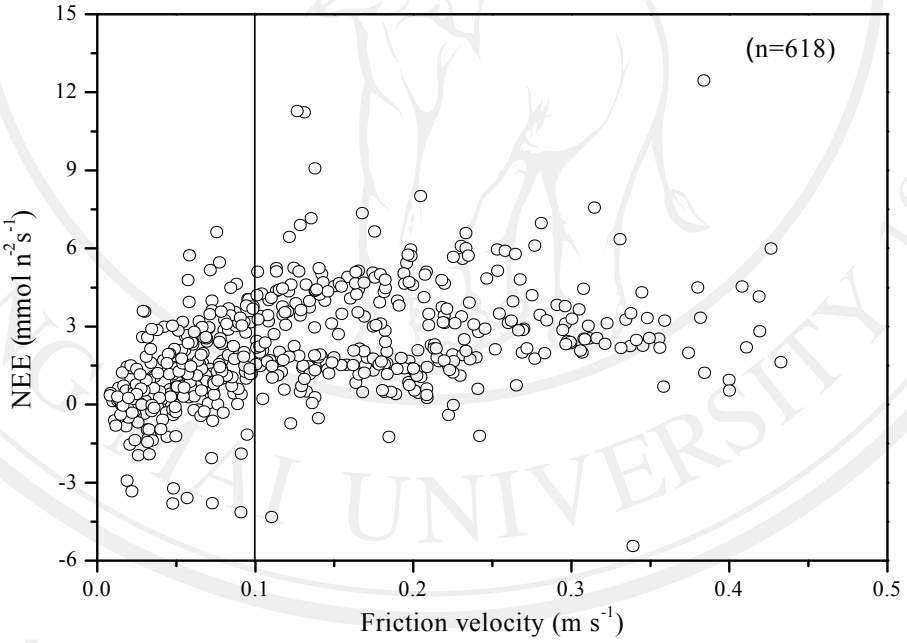

Figure 2.12 The nighttime net ecosystem exchange (NEE) versus the friction velocity in wheat field.

ลิขสิทธิ์มหาวิทยาลัยเชียงใหม่
Copyright© by Chiang Mai University
All rights reserved

Energy budget closure

Eddy covariance data quality was also assessed by analyzing the energy balance. The energy balance closure test provides only an indirect validation of CO_2 measurements. The good degree of energy balance closure suggests the good quality of CO_2 measurements. Energy balance closure was examined every 30 min by comparing the sum of latent and sensible heat flux (LE+H), measured by eddy covariance against available energy (Rn-G-S), measured by other methods, where H represents sensible heat flux, LE represents latent heat, Rn represents net radiation, G represents soil heat flux and S represents the heat storage in the soil layer above the heat flux plates. The 30 min values of LE+H was plotted against Rn-G-S. The linear regression was $(LE+H) = 0.83(Rn-G-S) + 38.1$, $R^2 = 0.88$, $P < 0.0001$. The slope value was close to 1, indicating that eddy fluxes were in approximate balance with the available energy (Fig. 2.13). Although, the energy balance closure is not perfect, it is within the normal range found in most studies. For the case of this study, part of the imbalance may be related to source scales of the measurements in Rn and G and to the loss of high-frequency fluctuations for water vapor.

ลิขสิทธิ์มหาวิทยาลัยเชียงใหม่
Copyright© by Chiang Mai University
All rights reserved

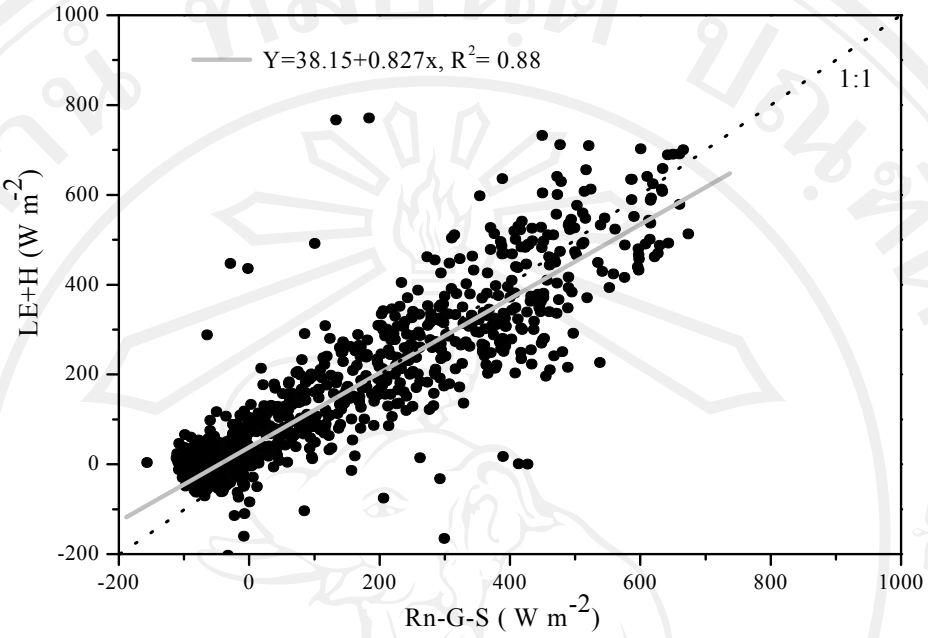

Figure 2.13 Energy balance closure at half-hourly scale in winter wheat growth period. Eddy covariance energy fluxes (LE+H) against available energy (Rn−G-S).

Statistical analysis and calculation

Multiple regressions and uncertainty analysis were calculated using the statistical software package Origin 7.0 to assess the relationship of NEE with concurrent changes in the environmental variables (net radiation, soil temperature and moisture). Daytime NEE was correlated with the net radiation using the Michaelis-Menten equation (Michaelis and Menten, 1912).

$$F_{NEE\,day} = \frac{-a' R_g}{1-(R_g/1000)+(a' R_g / F_{GPP,opt})} + F_{RE,day} \quad (1)$$

ลิขสิทธิ์มหาวิทยาลัยเชียงใหม่
Copyright© by Chiang Mai University
All rights reserved

where R_g is the net radiation (MJ m^{-2}) and the fitted parameters are $F_{RE,day}$, the ecosystem respiration during day time (μmol CO_2 m^{-2} s^{-1}), a', the ecosystem quantum yield (μmol CO_2 J^{-1}) and $F_{GPP,opt}$, the optimum *GPP* (μmol CO_2 m^{-2} s^{-1}) at an R_g value of 1000 MJ m^{-2}.

Nighttime NEE or ecosystem respiration (Re) was correlated with temperature using exponential equation.

$$F_{,night} = ae^{bT} \quad (2)$$

where $F_{,night}$ is nighttime *NEE*, *a* and *b* are fitted parameters, and T is temperature

To discuss the seasonal variation of photosynthetic activity, gross primary productivity (GPP) was obtained by the following equation using the observed NEE and estimated ecosystem respiration (Re). GPP was calculated as the difference between Re and NEE

$$F_{GPP} = -F_{NEE} + Re \quad (3)$$

ลิขสิทธิ์มหาวิทยาลัยเชียงใหม่
Copyright© by Chiang Mai University
All rights reserved

RESULTS

Information on weather conditions, biomass and leaf area

Meteorological conditions in winter wheat during growing season are given in Fig. 2.14. The maximum daily air and soil temperature occurred in DOY 130 (~27°C) and minimums occurred in DOY 20 to DOY 40 (~7°C) in wheat field (Fig. 2.12a). Total precipitation during wheat study period was 280.9 mm. Seasonal variation in soil volumetric water content followed the rainfall pattern and varied between 0.10 to 0.25 m^3m^{-3}. Green leaf area index (GLAI) began to increase significantly approximately 75 days after planting in wheat. During the period of most rapid canopy growth, the peak value of GLAI was 2.97 m^2m^{-2} (Fig. 2.15). Likewise, the aboveground biomass of wheat began to increase approximately 100 days after planting and the peak value was 0.94 kg DM m^{-2} (Fig. 2.15a).

ลิขสิทธิ์มหาวิทยาลัยเชียงใหม่
Copyright© by Chiang Mai University
All rights reserved

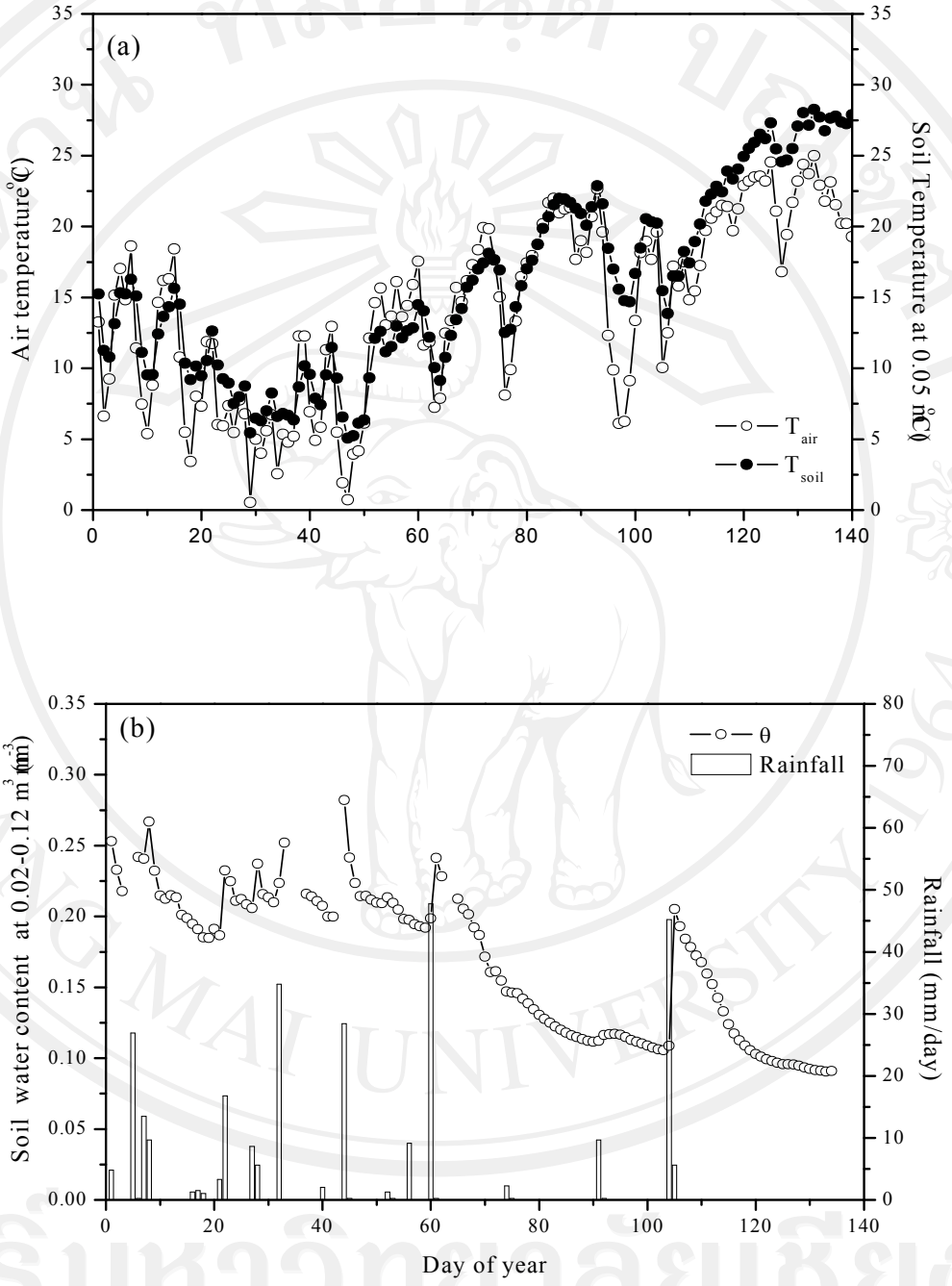

Figure 2.14 Daily mean air temperature, soil temperature and soil water content in the upper soil layer with rainfall during wheat growing seasons in 2007.

ลิขสิทธิ์มหาวิทยาลัยเชียงใหม่
Copyright© by Chiang Mai University
All rights reserved

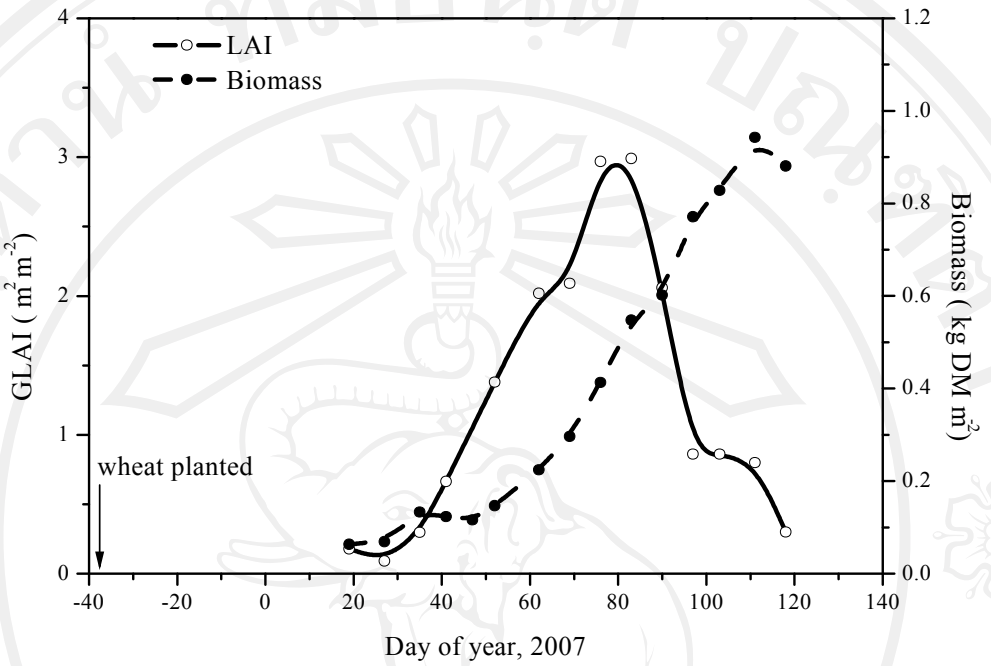

Figure 2.15 Seasonal distributions of green leaf area index (GLAI) and aboveground biomass of the winter wheat.

Diurnal change of CO_2 efflux (NEE) in the growing season

There was large seasonal variation in ecosystem photosynthetic and respiration activity as illustrated in the average diurnal patterns of NEE during wheat growing season (Fig. 2.16). The half hour data were averaged from 0:00 to 23:00 per biweekly periods in wheat growing seasons. The all data were divided into eight periods in wheat growing seasons. The average diurnal variations in NEE for each half hour are shown daytime CO_2 uptake and nighttime CO_2 release. The diurnal variation patterns of daytime uptake and nighttime release are evident in a wheat field. Before morning (7:00) the NEE moves from a positive value (release) to a negative value (uptake). The daytime uptake rate is highest around noon (13:00), and

ลิขสิทธิ์มหาวิทยาลัยเชียงใหม่
Copyright© by Chiang Mai University
All rights reserved

afterwards it begins to decrease. NEE during the early vegetative stage (DOY 1- 14) fluctuated within ± 5 μmol m^{-2} s^{-1}. The amplitude of the diurnal variation in NEE increased with the growth of wheat from seeding to flowering stage and reached maximum in the flowering period (DOY 71-84) , had maximum of NEE of - 37.5 μmol m^{-2} s^{-1}. During the grain filling stage, wheat field was converted to a CO_2 sink during two-thirds of the day. In the ripening period (DOY 99-112), daytime uptake decreased drastically, whereas nighttime release stay almost the same site as it was in the mid-vegetative stage.

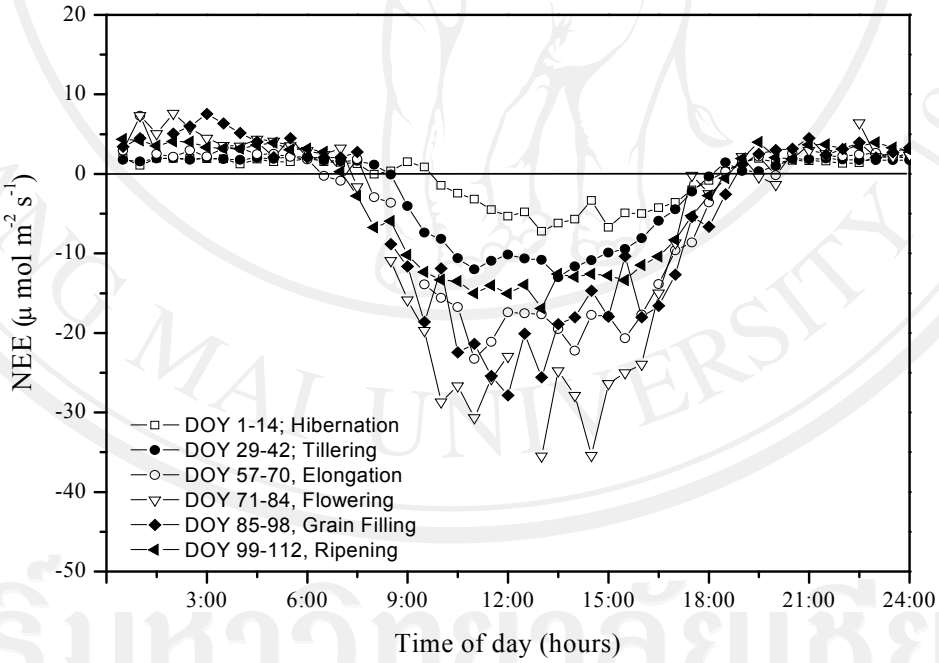

Figure 2.16 Diurnal variations of 14-day average net ecosystem exchange of CO_2 (NEE) in winter wheat field. Positive sign indicates carbon source while negative sign indicates carbon sink.

ลิขสิทธิ์มหาวิทยาลัยเชียงใหม่
Copyright© by Chiang Mai University
All rights reserved

Response of daytime NEE to incoming global radiation

To assess the response of daytime NEE to net solar radiation, Fig. 2.17 shows the light-response curve for short periods of the main stage of plant growth. More than 65% of the variation in NEE was explained by the change in net solar radiation. The daytime NEE increased along with net solar radiation and increased as LAI increases when compared with the same values of net solar radiation. The low NEE at the early season (DOY 1-14) was most like due to small canopy size, low temperature, and immature leaves. The NEE reached saturation at values ranging between -15 and -25 μmol m^{-2} s^{-1} when net solar radiation was approximately 700 W m^{-2} in the period of DOY 85-98 associated with the highest LAI.

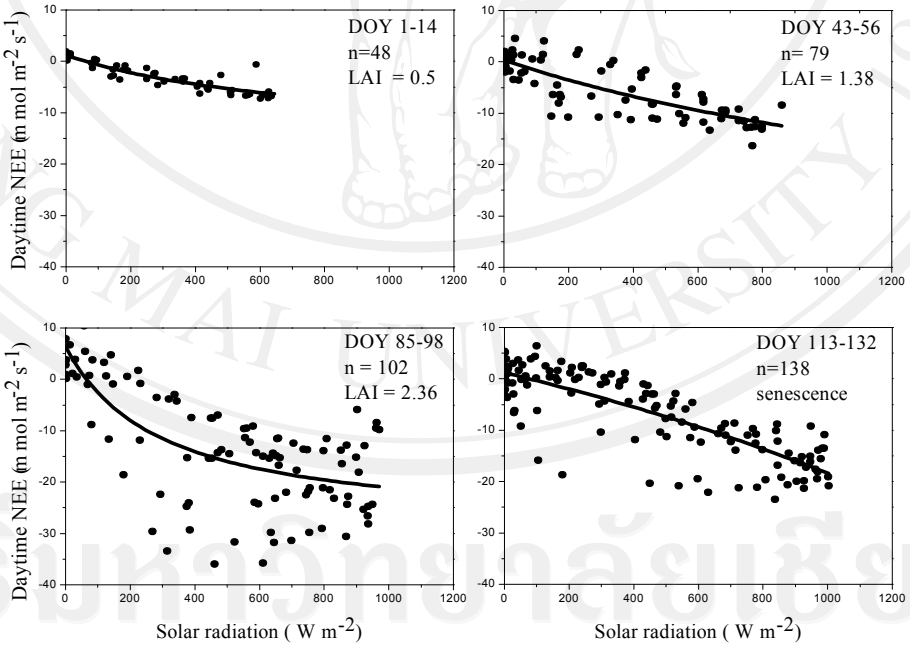

Figure 2.17 Example of light-response curves of daytime NEE at different growth stages of wheat growing season. Fitted curves are rectangular hyperbolic as described in Equation 1.

ลิขสิทธิ์มหาวิทยาลัยเชียงใหม่
Copyright© by Chiang Mai University
All rights reserved

Variation in net solar radiation was the primary control on diurnal variation in NEE. However, a distinct hysteresis was observed in the light response for NEE between morning and afternoon on day before (DOY 103) and after rainfall event (DOY 106) (Fig 2.18). The NEE at a give PAR was greater in the morning than in the noon, although no clear the ecosystem light compensation point for NEE was evident in this period, suggesting the stomatal regulation of carbon uptake. This resulted in significant hysterresis in the relationship between NEE and PAR. On day before rainfall, as PAR increased in the morning, NEE increased, reaching the peak value at PAR of 1000 μmol photons m^{-2} s^{-1} and then rapidly decreased. As PAR decreased, NEE decline slightly throughout the afternoon. On day after rain, as PAR increased in the morning, NEE increased (gets more negative) and as PAR decreased in the afternoon, NEE declined. Additionally, the diurnal patterns in soil temperature and soil water content were similar for the two days but different in magnitudes. The NEE was more negative, indicating greater CO_2 uptake, in day after rainfall compared with the day before rainfall. A hysteresis loop found in their relation indicated that there is a difference in the exchange behavior of these gases between day before and after rainfall. Assuming that changes in soil temperature and soil water content by rainfall would tend to increase in NEE and was dominant control in the NEE-PAR response.

ลิขสิทธิ์มหาวิทยาลัยเชียงใหม่
Copyright© by Chiang Mai University
All rights reserved

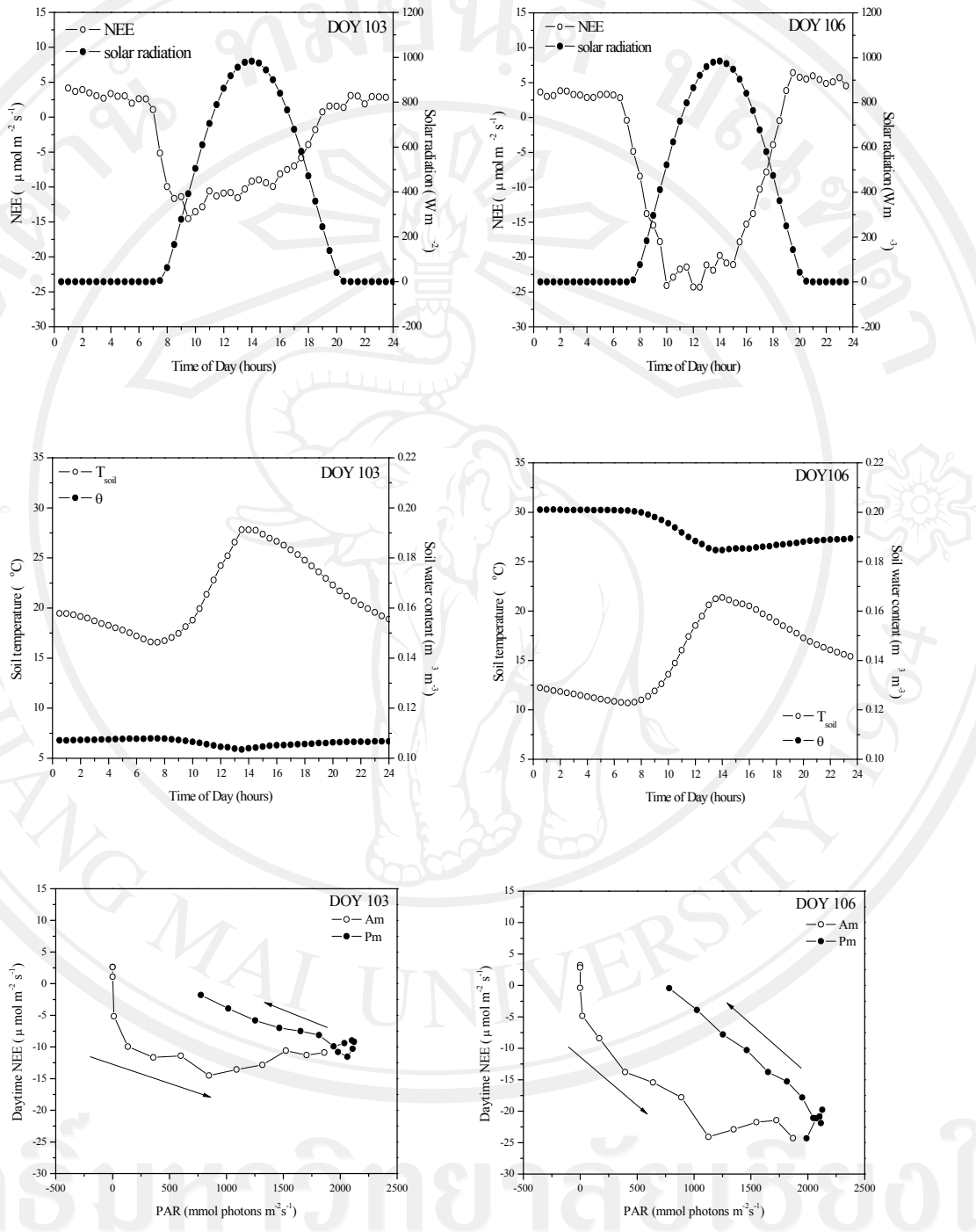

Figure 2.18 Diurnal variations of NEE, solar radiation, soil temperature and volumetric soil water content on days before 50.8mm-rainfall event (DOY 103) and on day after rainfall (DOY 106). The relationship between PAR and daytime NEE during morning (6:00 – 12:00) and afternoon (12:30 – 18:30) periods.

ลิขสิทธิ์มหาวิทยาลัยเชียงใหม่
Copyright© by Chiang Mai University
All rights reserved

Response of gross primary production (GPP) and nighttime NEE to biophysical and environmental factors

Measurements of NEE were used to estimate gross primary production (GPP). The GPP or carbon assimilation is the result of several interacting factors, including temperature, soil water content, radiation and LAI. Soil temperature and soil water content explained about 32% and 40% of the variation in daily GPP (Fig. 2.19). The GPP responded linearly to changes in LAI and aboveground biomass (Fig. 2.20 and 2.21). Over 94% and 82% of the variation were explained by change in LAI and aboveground biomass, respectively. The 16% and 18% of variance was due to variations in the other weather/soil variables, such temperature, soil water content and direct radiation. During the late reproductive stages, the relationship between the GPP and aboveground biomass seemed to have little changed. In general, GPP increased by about 7.66 μmol m^{-2} s^{-1} per day for each incremental increases in LAI.

The relationship between half-hourly nighttime NEE or ecosystem respiration (Re), which are equivalent to ecosystem respiration, and canopy temperature was well described by exponential function (Table 2.3). Canopy air temperature explained 50% of the variation in ecosystem respiration (Fig. 2.21). The relationship between ecosystem respiration and canopy air temperature gave a base respiration rate of 1.70 μmol m^{-2} s^{-1} and Q_{10} was 1.93. The relationship between ecosystem respiration and soil water content between 0.02-0.08 depths was weak. The relationship between ecosystem respiration and soil water content was described by quadratic function and explained only 25% of the variation in ecosystem respiration (Fig. 2.24).

Data from the eddy covariance measurements were compared to soil respiration data collected simultaneously using soil CO_2 gradient measurements.

ลิขสิทธิ์มหาวิทยาลัยเชียงใหม่
Copyright© by Chiang Mai University
All rights reserved

Fig. 2.25 shows the impact of one such event on ecosystem and soil respiration after 33 days with out rainfall. The soil respiration and ecosystem respiration datasets demonstrated an elevated respiration rate on the day following the rainfall. Soil respiration and ecosystem respiration showed an increase of 0.21 and 0.01 times pre rainfall rate. In DOY 67-75 and DOY 76-90, soil respiration comprised 65% and 62% of ecosystem respiration. On the day following rainfall, soil respiration comprised 51% of ecosystem respiration.

ลิขสิทธิ์มหาวิทยาลัยเชียงใหม่
Copyright© by Chiang Mai University
All rights reserved

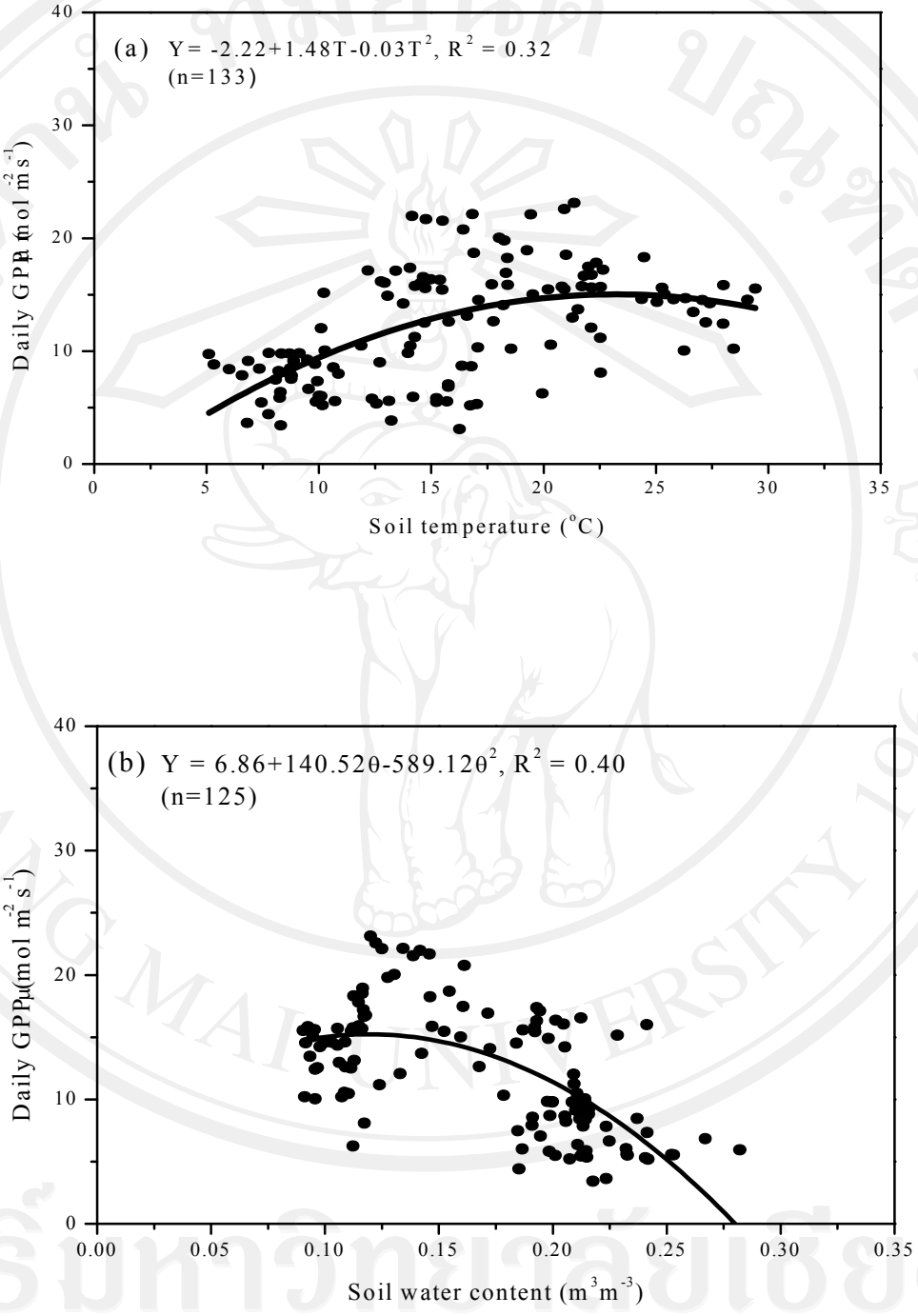

Figure 2.19 The responses of daily gross primary production (GPP) to soil temperature (a) and soil water content (b).

ลิขสิทธิ์มหาวิทยาลัยเชียงใหม่
Copyright© by Chiang Mai University
All rights reserved

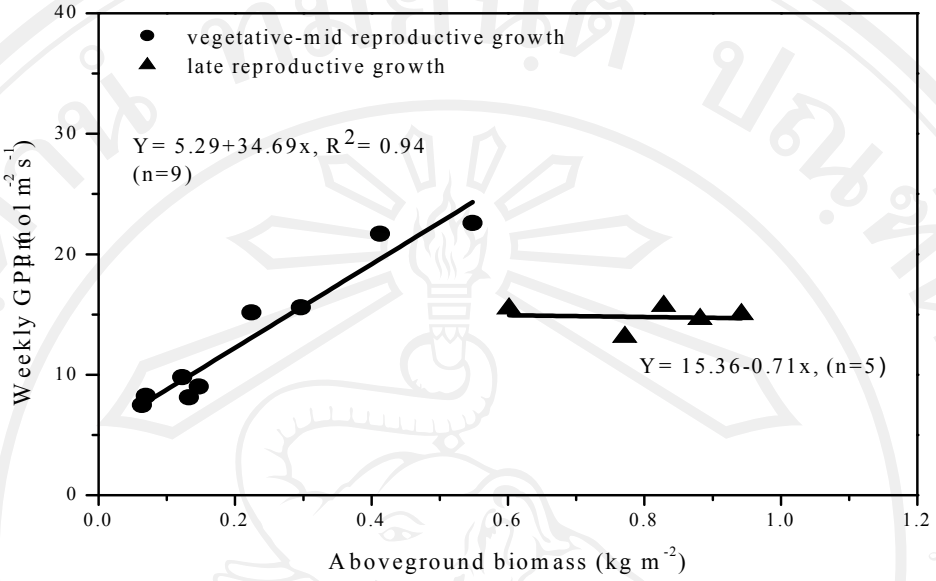

Figure 2.20 Relationship between gross primary production (GPP) and aboveground-biomass. Weekly averages of half-hours are plotted.

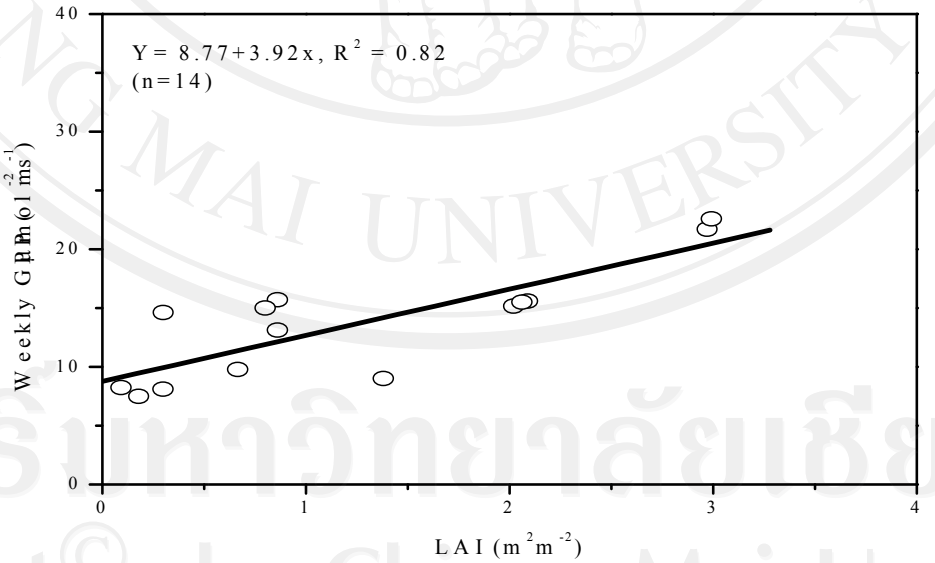

Figure 2.21 Relationship between gross primary production (GPP) and leaf area index (LAI). Weekly averages of half-hours are plotted.

ลิขสิทธิ์มหาวิทยาลัยเชียงใหม่
Copyright© by Chiang Mai University
All rights reserved

Table 2.3 Nonlinear regression results of ecosystem respiration models

Temperature Factor	a	b	R^2	Q_{10}
Air temperature	1.56	0.065	0.47*	1.91
Canopy air temperature	1.70	0.066	0.50*	1.93
Soil temperature	1.32	0.060	0.46*	1.82

*a, b, c, d are significant coefficients ($\alpha < 0.05$). R^2 stands for determination coefficient. All models are significant ($\alpha < 0.05$).

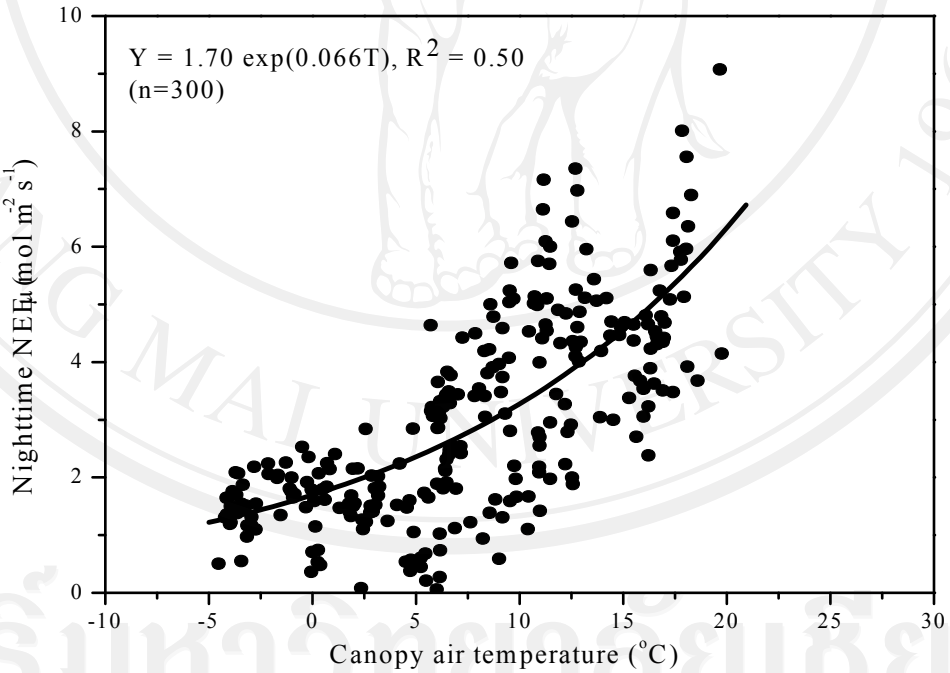

Figure 2.22 Response of half-hourly ecosystem respiration to changes in canopy air temperature.

ลิขสิทธิ์มหาวิทยาลัยเชียงใหม่
Copyright© by Chiang Mai University
All rights reserved

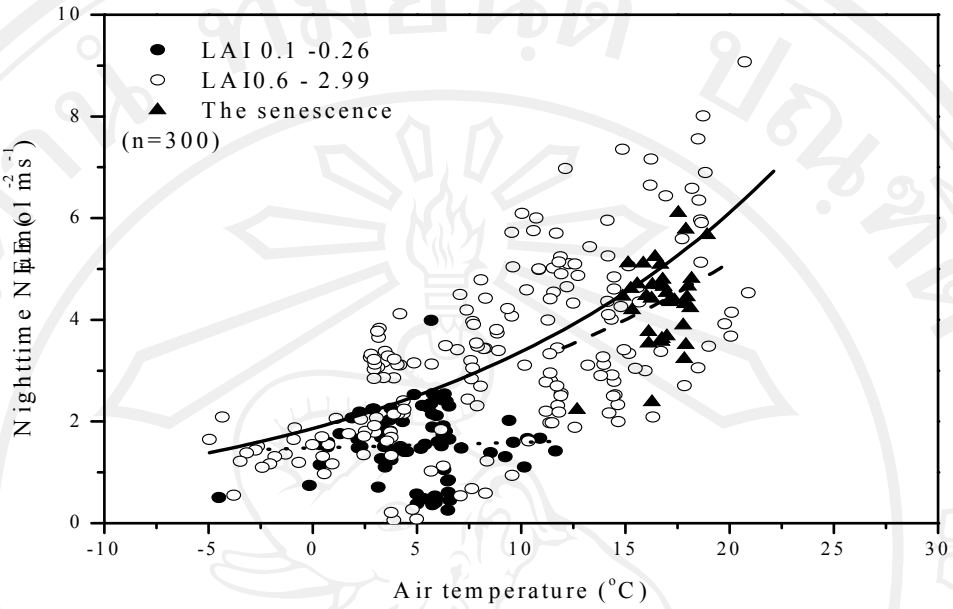

Figure 2.23 Response of half-hourly ecosystem respiration to changes in air temperature for difference periods in the growing season.

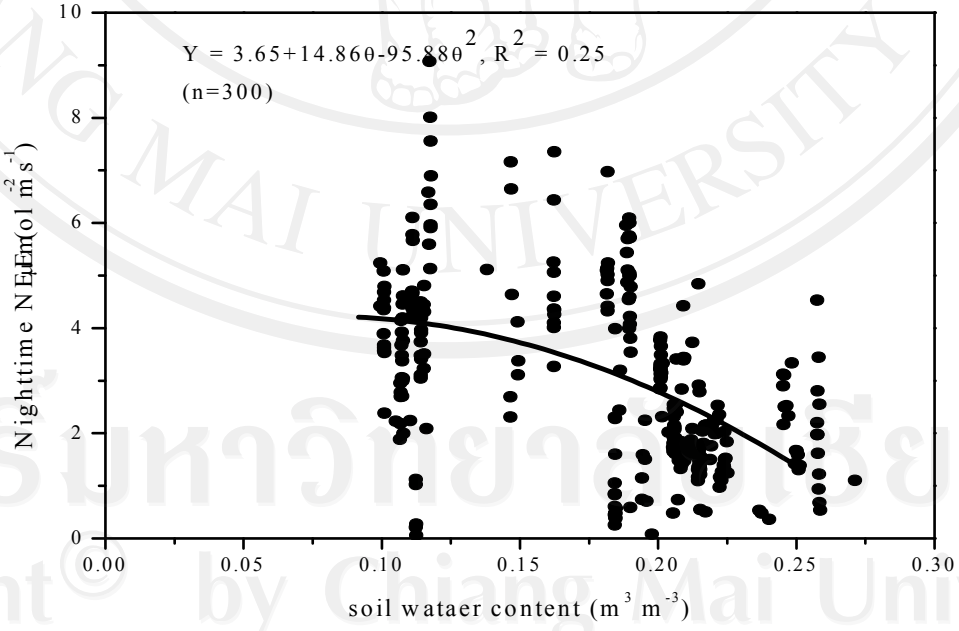

Figure 2.24 Response of half-hourly ecosystem respiration to changes in soil water content.

ลิขสิทธิ์มหาวิทยาลัยเชียงใหม่
Copyright© by Chiang Mai University
All rights reserved

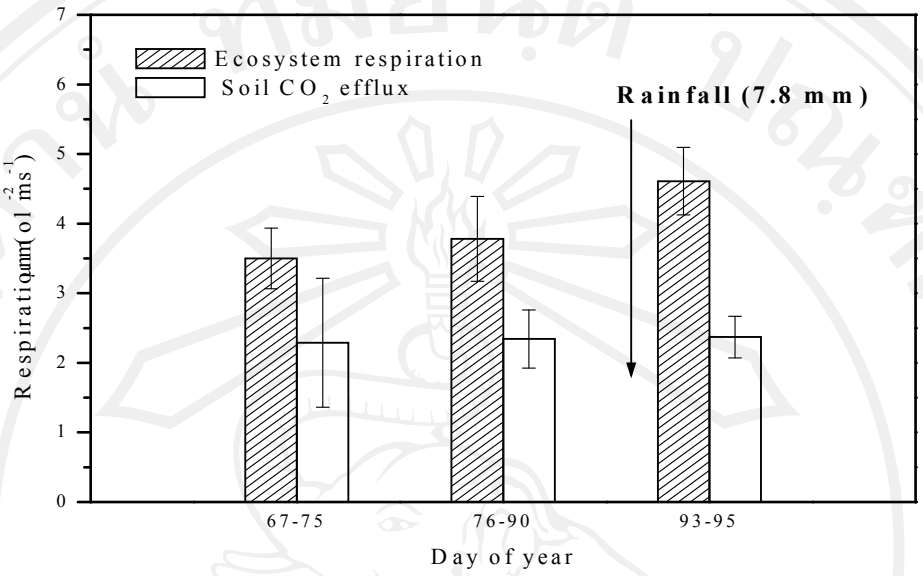

Figure 2.25 Average soil respiration measured using soil gradient measurement and daily average ecosystem respiration prior to and following a rainfall event.

ลิขสิทธิ์มหาวิทยาลัยเชียงใหม่
Copyright© by Chiang Mai University
All rights reserved

DISCUSSION

Daytime NEE influenced by biophysical and environmental factors

In the growing season, peak of CO_2 uptake or negative daytime NEE was reached during DOY 71-84 (mid-March), which corresponded to winter wheat tillering (Fig 2.16). This rapid rate of CO_2 uptake coincided with maximum LAI. From late March to ending of growing season, the daytime NEE decreases due to the LAI decrease. These results were consistent with the results of Moureaux *et al.* (2008) in Belgian winter wheat crop. The daytime NEE at a give net solar radiation was lower in the afternoon than in the morning (Fig. 2.17). The less negative daytime NEE during the afternoon appeared to be caused by lower photosynthetic rate and enzyme activity at high temperature and atmospheric vapour pressure deficit (VPD). The highest soil temperature in the afternoon probably induced a shout down of photosynthesis through partial stomatal closure. High temperatures are typically accompanied by high atmospheric vapour pressure deficit. Farquhar and Sharkey (1982) reported that high VPD could strong limit photosynthesis through stomata closure. In addition to the stomatal limitation, Fu *et al*. (2006) inferred that high temperature at midday caused the NEE reduction through a decrease of photosynthesis an increase of ecosystem respiration.

On half-hour time scale, solar radiation was the primary physical variable controlling daytime NEE (Fig. 2.18), accounting for 45 to 78 % variations of NEE during growing season. But this daytime NEE- net solar radiation relationship was modulated by LAI. Daytime NEE is the result of several interacting factors, including temperature, rainfall, solar radiation and leaf area index (LAI) (Carrara *et al.,* 2004;

ลิขสิทธิ์มหาวิทยาลัยเชียงใหม่
Copyright© by Chiang Mai University
All rights reserved

Zhang *et al.,* 2007; Fawei *et al.,* 2008). A study on grassland demonstrated that NEE and GPP responded to LAI in a linear manner and 84% of the variance in GPP could be explained by the variation in LAI (Aires *et al.,* 2008). Carbon assimilation in wheat plant is the result of several interactions such as temperature, soil moisture, biomass and LAI. Among these factors, there were relationships to some extent the aboveground biomass, LAI and GPP in this study. The linear relationship was positive with GPP. It was suggested that the augment of aboveground biomass and LAI enhanced the carbon sequestration capacity of the ecosystem. The influence of the aboveground biomass on GPP was greater than that of the LAI.

Nighttime NEE influenced by environmental factors

Nighttime NEE or ecosystem respiration consists of both autotrophic (plant) and heterotrophic respiration (microbial decomposition). Generally, temperature and soil moisture have been documented as the primary controlling factors of ecosystem respiration studies in wide range of ecosystem. The ecosystem respiration was co-affected by multiple environmental factors such as air temperature, soil temperature, canopy temperature and soil moisture. Nighttime data were used and an exponential model was used fitted in this study. Results showed that canopy temperature was a main factors affecting ecosystem respiration. The Q_{10} value was 1.93. Pattey *et al.* (2002) obtained similar results in rainfed maize using nighttime averages ecosystem respiration. Their Q_{10} values ranged from 1.6 to 2.2. Suyker *et al.* (2005) found the relationship between ecosystem respiration and air temperature. Their Q_{10} values ranged from 1.3 to 1.4 for rainfed maize and from 1.3 to 1.6 for rainfed soybean. It is likely that the plant biomass in crop field exhibit large seasonal

ลิขสิทธิ์มหาวิทยาลัยเชียงใหม่
Copyright© by Chiang Mai University
All rights reserved

changes, which also affect ecosystem respiration. It is important to consider other biophysical factors such as leaf area and plant biomass affect ecosystem respiration (Suyker *et al.,* 2004; Saito *et al.,* 2005). In this study, nighttime NEE was considerably larger in the second part of season (LAI = 0.6-2.19) compared with the first part (early stage, LAI = 0.1-0.26) (Fig 2.19). The nighttime NEE at first part and third part (senescence period) showed weak relationship to air temperature. In contrast, during the second part of growing season, the relationship to air temperature seemed strong. Moureaux *et al.* (2008) observed similar behavior of ecosystem respiration in a winter wheat. Early in the season, the lack of temperature response may be due to small values of biomass and LAI, small ranges of air temperature and significant contribution of soil respiration. Also noted from Fig. 2.23 is that nighttime NEE during the second part was high sensitive to change in air temperature, reflecting importance of photosynthetic activity which stimulated by increase in air temperature. With the onset of senescence, nighttime NEE was less temperature-sensitive. This indicated that the ecosystem respiration in the late growing period was dominated by plant maintenance respiration. Changing phenology (e.g. leaf area and biomass) play an important role in controlling ecosystem respiration. The amount of ecosystem respiration also differed among the soil moisture conditions: ecosystem respiration declined with increasing volumetric water content, although this relationship was not strong. Consistent with the result of Gaumont-Guay *et al.* (2006) and Wang *et al.* (2008), they reported that high soil water content limited soil respiration, resulting in low ecosystem respiration. This could be explained by lessening of oxygen availability for microbial activity due to a soil porosity reduction as high soil water

ลิขสิทธิ์มหาวิทยาลัยเชียงใหม่
Copyright© by Chiang Mai University
All rights reserved

content. Davidson *et al.* (2000) concluded that the soil respiration decreased at soil water content either higher or lower.

Several studies have reported large increases of ecosystem respiration (Re) immediately after a rainfall event based on forest field measurements (Xu and Baldocchi, 2004; Jarvis *et al*., 2007). Several researchers indicated that Re suddenly increased following rainfall due to the quick activation of soil microbial respiration, with the consequent mineralization of organic matter and nutrient and activation of plant growth (Birch, 1958; Xu *et al.,* 2004; Aires *et al.,* 2008). Kielgaard *et al*. (2008) also found that net carbon uptake during the daytime increased following both low and high variable rainfall. Although, Nakano *et al.* (2008) found that increase of soil water content after rainfall caused an increase in the respiratory release of CO_2, but the photosynthetic uptake of CO_2. In this study the amount of Re was large when soil water content was a little high, which occurred after a rainfall event and rainfall event had no effect on soil respiration (Fig. 2.25). The high values of Re observed after the rainfall event must be explained by this affect as the small rainfall event led to enhance wheat growth. This increases in Re in this study due to increases in soil water content after rain, resulting in stimulation in wheat growth.

In summary, at the beginning of the growing season (in January), low temperature and young wheat limited carbon assimilation (daytime NEE) and respiration of ecosystem. In addition, ploughing altered soil structure in wheat field which not only drove higher release rates of soil respiration, but also exposed previously physically protected soil organic carbon for consumption by microorganism. With temperature increases and wheat development, carbon assimilation and respiration were significantly elevated. However, carbon assimilation

ลิขสิทธิ์มหาวิทยาลัยเชียงใหม่
Copyright© by Chiang Mai University
All rights reserved

was limited greatly when temperature and net solar radiation increased beyond certain levels. Carbon assimilation was limited around noon and early afternoon. Carbon assimilation was linearly related to amount of above ground biomass. At the given growth stage, the daytime NEE and net radiation was closely linked through a hyperbolic relationship. Ecosystem respiration followed the exponential function of canopy temperature. The large increase in ecosystem respiration after rainfall, especially those in the dry period was also observed.

ลิขสิทธิ์มหาวิทยาลัยเชียงใหม่
Copyright© by Chiang Mai University
All rights reserved